

LENGTHENED G1 PHASE INDICATES DIFFERENTIATION STATUS  
IN HUMAN EMBRYONIC STEM CELLS.

A LENGTHENED G1 PHASE INDICATES DIFFERENTIATION STATUS  
ACROSS MULTIPLE LINEAGES IN HUMAN EMBRYONIC STEM CELLS.

By ASHLEY CALDER, B. Sc.

A Thesis Submitted to the School of Graduate Studies in Partial Fulfilment of the  
Requirements for  
the Degree Master of Science

MASTER OF SCIENCE, 2011; BIOCHEMISTRY AND BIOMEDICAL  
SCIENCES;

McMASTER UNIVERSITY, Hamilton, Ontario

TITLE: A lengthened G1 phase indicates differentiation status across multiple  
lineages in human embryonic stem cells.

AUTHOR: Ashley Calder, B.Sc.

SUPERVISOR: Dr. Jon Draper

NUMBER OF PAGES: *vii*, 54

## **Abstract**

Human embryonic stem cells (hESC) have potential applications as tools for drug screening to identify small molecule regulators of self-renewal or differentiation. Elucidating the mechanisms governing lineage commitment in hESC will allow for efficient derivation of specified cell types for clinical use. Recognizing the early steps in loss of pluripotency is key to achieving both goals of drug screening and derivation of therapeutically relevant cell types. Here we report the use of a real time cell cycle fluorescent reporter for the first time in hESC that indicates onset of differentiation in a lineage unbiased manner. Pluripotent hESC possess a short cell cycle length, due primarily to a truncated G1 phase. G1 lengthens concomitant with differentiation. Stable hESC lines expressing the live cell cycle reporter exhibit fluorescence only during G1. Due to the short length of pluripotent G1 phase, G1 fluorescence is only weakly and transiently detected, however it is quickly increased to easily detectable levels upon onset of differentiation. We hypothesize that lengthened G1 phase can be used as an indicator of differentiation status of individual human embryonic stem cells.

Cells with lengthened G1 are typically negative for pluripotency markers OCT4, Tra-1-60 and SSEA-3 following differentiation. Differentiated cells with lengthened G1 also demonstrate increased levels of lineage-specific differentiation markers at both the protein and mRNA level. Automated image analysis of hESC indicates this mutually exclusive relationship between lengthened G1 and pluripotency exists both on the cellular level and in colonies as a whole. Here we have shown that lengthened G1 indicates both loss of pluripotency and gain of lineage markers.

## Acknowledgements

The work embodied in this thesis could not have been achieved without the wonderful support and help from many valuable members of the McMaster Stem Cell and Cancer Institute (SCCRI) and Biochemistry & Biomedical Sciences department.

I am greatly appreciative of the research associates, talented technicians, and staff for sharing their talents and time. Great thanks to **Dr. Marilyn Levadoux-Martin** for instruction in flow cytometry operation and analysis and FACS; **Jennifer Russell** for ArrayScan operation; **Jamie McNicol** for fluorescent microscope and imaging support and analysis, and Biostation operation support; and **Dr. Tony Collins** for image analysis support, script development and writing for Accapella and MatLab.

I am grateful to the kind and generous support I received from my colleagues in the SSCRI. Thank you to **Dr. Chitra Venugopal, Nicole McFarlane, Monica Graham, Zoya Shapovalova, and Monika Malig** for all of your kind words, encouragement, and friendly smiles when I needed them. A very special thanks to Doble lab members **Dr. Kevin Kelly** and **Deborah Ng**. Kevin, thank you for always willingly sharing your time and expertise in the lab and providing both personal and academic direction and advice. Deb, graduate school would not have been nearly so enjoyable without your friendship.

I admire and appreciate my committee members **Dr. Ray Truant** and **Dr. Brad Doble** for their time, involvement, and direction provided during the course of my studies. Thanks to Ray for his vast knowledge of imaging, all things fluorescent, and for attempting to raise my awareness of caveats in my research. I am especially appreciative to Brad for his continual support, for always being available to talk and listen. Thank you for being the first person at McMaster to encourage me to pursue graduate studies, and for continuing to provide that encouragement.

I am fortunate to have been given the option to research and study in the Draper lab. Thank you to my two lab mates, **Dr. Carlos Pilquil** and **Ivana Roth-Albin** for all you have done. Thank you to my supervisor, **Dr. Jon Draper** for inviting me into his lab and providing space and funding to work. I am indebted to you for sharing your talents and teaching me the valuable skills of cloning and hESC culture.

And most of all, thank you to my entire family, because you believed I could do it all, when I knew I could not.

## Table of Contents

### Introduction

Cell cycle, differentiation, and development .....	1
G1 regulation and fate decisions .....	2
Expression of G1 regulatory molecules in human embryonic stem cells .....	4
Live fluorescent cell cycle reporter .....	8
Differentiation of human embryonic stem cells .....	8
Human embryonic stem cells and screening .....	11

### Methods

Cell culture .....	13
Generation of reporter constructs .....	13
Generation of stable reporter hESC lines .....	13
Time lapse imaging .....	14
Differentiation .....	14
Flow cytometry .....	15
FACS .....	15
Indirect immunofluorescence .....	15
Image analysis .....	16
RT-qPCR .....	17
Colony initiating cell assay .....	17

### Results

Generation of human embryonic stem cell lines stably expressing a cell cycle reporter .....	19
Validation of G1-exclusive expression of Fucci Orange reporter .....	20
Differentiating hESC show increased Fucci Orange expression .....	27
Lengthened G1 indicates loss of pluripotency .....	30
Lengthened G1 indicates gain of lineage markers .....	34

### Discussion

Use of Fucci Orange in hESC .....	37
Lengthened G1 indicates loss of pluripotency .....	38
Lengthened G1 indicates gain of lineage .....	40
Caveats and considerations .....	41
Future work .....	42

<b>References</b> .....	<b>44</b>
-------------------------	-----------

## List of Figures

<b>Figure 1:</b> Early human embryonic development includes significant changes in cell cycle features.....	2
<b>Figure 2:</b> Expression profiles of active cell cycle regulators.....	5
<b>Figure 3:</b> Image analysis workflow .....	17
<b>Figure 4:</b> Fucci Orange reporter constructs and expression pattern .....	19
<b>Figure 5:</b> Cyclin B1 is not expressed in Fucci Orange positive cells .....	22
<b>Figure 6:</b> Fucci Orange and SKP2 are co-expressed in a subset of hESC.....	23
<b>Figure 7:</b> Fucci Orange and SKP2 expression are not mutually exclusive in undifferentiated hESC .....	24
<b>Figure 8:</b> Expression pattern of SKP2 sensor .....	26-27
<b>Figure 9:</b> Fucci Orange expression increases under differentiation conditions and is dose-dependent .....	28-29
<b>Figure 10:</b> Fucci Orange-positive cells are more likely to be OCT4-negative.....	30
<b>Figure 11:</b> Fucci Orange positive cells are more likely to be negative for pluripotency-related cell surface markers SSEA-3 and Tra-1-60 .....	31
<b>Figure 12:</b> OCT4 positive cells are more likely to be Fucci Orange-negative .....	31
<b>Figure 13:</b> Automated colony analysis reveals an inverse relationship between Fucci Orange expression and OCT4 across entire colonies .....	32
<b>Figure 14:</b> Fucci Orange expression is correlated with a change in gene expression of pluripotent and differentiation markers.....	33
<b>Figure 15:</b> Fucci Orange negative hESC populations contain more colony –initiating cells.....	34
<b>Figure 16:</b> Fucci Orange expression correlates with a gain of lineage-related gene expression .....	35
<b>Figure 17:</b> Endoderm markers are more likely to be Fucci Orange-positive.....	36

## List of Abbreviations

<b>CDK:</b>	Cyclin-dependent kinase
<b>CIC:</b>	Colony-initiating cell
<b>CKI:</b>	Cyclin-dependent kinase inhibitor
<b>DMSO:</b>	Dimethyl sulfoxide
<b>ESC:</b>	embryonic stem cell
<b>FACS:</b>	Fluorescent activated cell sorting
<b>G1 phase:</b>	Gap 1 phase
<b>G2 phase:</b>	Gap 2 phase
<b>H2GFOIP:</b>	CAG-H2B GFP F2A Fucci Orange IRES Puro
<b>HCS:</b>	High content screening
<b>hECC:</b>	human embryonal carcinoma cell
<b>hESC:</b>	human embryonic stem cell
<b>HMBA:</b>	hexamethylene bisacetamide
<b>HTS:</b>	High-throughput screening
<b>iPSC:</b>	induced pluripotent stem cell
<b>IVF:</b>	in vitro fertilization
<b>M phase:</b>	mitosis phase
<b>MEF:</b>	mouse embryonic fibroblast
<b>MEL:</b>	murine erthyroleukemia cell
<b>mESC:</b>	mouse embryonic stem cell
<b>PI3K:</b>	phosphatidylnositol 3-kinase
<b>pRb:</b>	retinoblastoma protein
<b>RA:</b>	retinoic acid
<b>RAR:</b>	retinoic acid receptor
<b>RARE:</b>	retinoic acid receptor element
<b>S phase:</b>	synthesis phase

## **Declaration of Academic Achievement**

**Ashley Calder** created the expression vectors, all cell lines, and performed all experiments (except the CIC assay) and analyses.

**Jon Draper** provided funding, experimental design, and support. He also performed the CIC assay.

**Tony Collins** developed and wrote image analysis scripts for Columbus, Accapella, and MatLab.

**Jennifer Russell** wrote programming and images plates in the ArrayScan.

**Marilyn Levadoux-Martin** performed cell isolation via FACS.

## **Introduction**

### Cell cycle, differentiation, and development

Human embryonic stem cells (hESC) are defined by their ability to self-renew indefinitely in culture while maintaining the developmental potential to differentiate into any cell type representative of the adult body. A less commonly discussed defining characteristic of hESC is their unique cell cycle phase profile: total cell cycle length is only ~16 hours long, due primarily to a truncated G1 phase length of only ~3 hours<sup>1</sup>. G1 lengthens concomitant with the onset of differentiation, extending the duration of total cell cycle time. The coupling of differentiation and cell cycle changes are intrinsically linked throughout the development of many species. *Drosophila melogaster*<sup>2,3</sup>, *Xenopus laevis*<sup>4,5</sup>, zebrafish<sup>6</sup>, mouse<sup>7</sup>, rat<sup>8</sup>, and human early embryos<sup>9</sup> all demonstrate shortened cell cycle lengths with truncated gap phases that lengthen as development progresses. The developing human embryo undergoes successive mitosis (M) and synthesis (S) phases until the early morula stage is reached, when the first detectable gap phases occur. Activation of the embryonic genome occurs at the 8-cell stage<sup>10</sup>, immediately preceding the inclusion of the gap 1 (G1) phase in the embryonic cell cycle (Figure 1). Thus, there appears to be a temporal link between embryonic transcription, inclusion of G1, and the first fate decision made in the morula when cells trapped in the innermost portion of the embryo adopt an “inside” rather than “outside” identity. Inhibition of cell cycle expansion causes developmental defects in *Drosophila*<sup>2,11</sup>. Cell cycle length in 2-cell stage human embryos created for *in vitro* fertilization (IVF) has been shown as a reliable indicator of embryo developmental potential<sup>12</sup>. Together, these findings illustrate that strong linkages between cell cycle regulation and proper development are evolutionarily conserved.

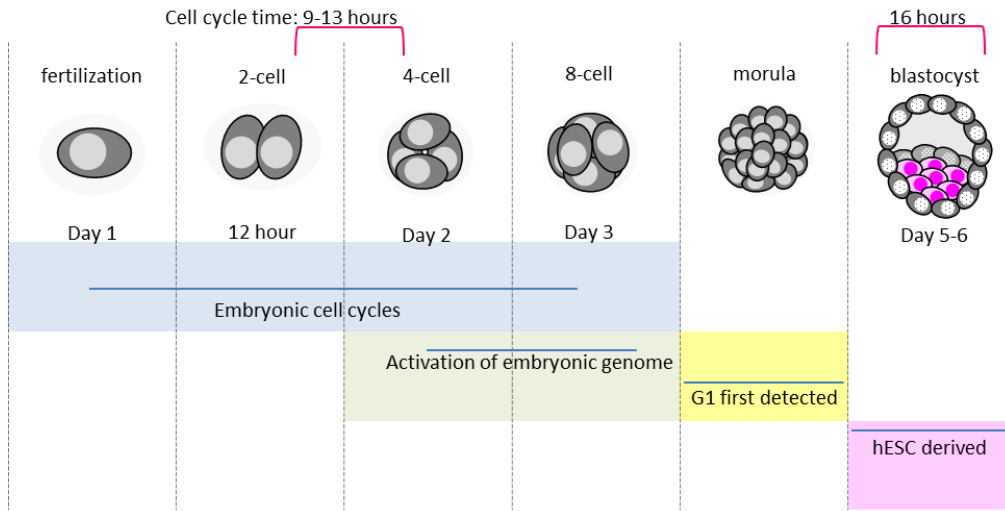


**Figure 1: Early human embryonic development includes significant changes in cell cycle features.** Cleavage times giving rise to the 4-cell stage are estimated at 9-13 hours to give rise to a healthy blastocyst. The first sets of embryonic cell cycles include only successive synthesis and mitosis phases. Activation of the embryonic genome occurs by the 8-cell stage. The first detectable G1 phase can be observed in the early morula. The epiblast (pink) of the blastocyst can be explanted to give rise to human embryonic stem cells *in vitro*.

Pluripotent embryonic stem cells (ESC) derived from peri-implantation stage blastocysts of mouse<sup>13</sup>, rat<sup>14</sup>, and human<sup>1</sup> maintain the shortened cell cycle phases found in the originating embryos. The contracted cell cycle profile found in embryonic stem cells is also shared by other human pluripotent cell types, human embryonal carcinoma cells (hECC)<sup>15</sup> and induced pluripotent stem cells (iPSC)<sup>16</sup>. Inhibition of cell cycle progression in fibroblasts transduced with established reprogramming factors (OCT4, SOX2, c-MYC, and KLF4) prevents reprogramming<sup>17</sup>, suggesting a mechanistic link between establishment of pluripotency and cell cycle control.

Adult stem and progenitor cells found in zebrafish<sup>18</sup>, *Drosophila*<sup>11</sup>, and mouse<sup>19</sup> share this same trend of maintaining an abrogated cell cycle which lengthens upon differentiation. Most work in this area has been carried out in neural systems, with studies of mouse neural stem cells suggesting that lengthening of G1 is causative of differentiation, not a result<sup>20,21</sup>. To date, the directionality of the relationship between lengthened G1 and differentiation has yet to be demonstrated in hESC.

### G1 regulation and fate decisions

The cell cycle is controlled by phase-specific sets of regulatory proteins, whose expression and function oscillate with the cell cycle. Because G1 is the cell cycle phase most strikingly altered during development and differentiation, we have

chosen to focus on changes in G1 phase length. G1 is regulated by the cyclins Cyclin E and Cyclin D1; the cyclin-dependent kinases (CDK) CDK2 and CDK4; the cyclin-dependent kinase inhibitors (CKI) p27 and p21; and the retinoblastoma protein (pRb).

G1 can be divided into two phases: early G1 when pRb is un/hypophosphorylated and active and late G1 when pRb is hyperphosphorylated and inactive. Inactivation of pRb by phosphorylation permits release of E2F family transcription factors that are normally bound by active pRb<sup>22</sup>, resulting in transcription of genes required for S-phase activities such as DNA synthesis<sup>23</sup>. The point dividing early from late G1, when pRb phosphorylation occurs, is referred to as the restriction point (R-point). Cyclin D1 forms a complex with CDK4 and acts in early G1 to phosphorylate pRb. Cyclin E complexes with CDK2 and phosphorylates pRb<sup>24</sup> in late G1. It is thought that Cyclin D1/CDK4 is required for transit through early G1 and Cyclin E/CDK2 is required for the G1-S transition. Both p21 and p27 can form inhibitory complexes with Cyclin D1/CDK4 and Cyclin E/CDK2. Although these G1 regulatory molecules do show cell cycle specific expression patterns, they are also actively degraded outside of G1 through ubiquitin-mediated proteolysis by the SCF<sup>Skp2</sup> ligase<sup>25,26</sup>. SKP2 is the E3 ligase component of the ubiquitin ligase responsible for marking target proteins with ubiquitin, resulting in eventual proteasome-based degradation. SKP2 recognizes targets and binds to them via F-box sequences, and conjugates a ubiquitin residue to the target protein. This initial ubiquitin molecule is then extended into a polyubiquitin chain by linking additional lysine molecules via the L42 residue in the previously-added ubiquitin. Following addition of a polyubiquitin chain to a target protein, the protein is then recognized and admitted into the proteasome complex for degradation.

G1 is known as a fate-decision making phase<sup>27-30</sup>. Modulation of cell cycle regulatory molecules that control G1 checkpoints and cell passage through G1 to S phase alter the ability of a cell to undergo apoptosis, enter or remain in quiescence, or differentiate. The differentiation process appears to be regulated primarily by p21 and p27. In oligodendrocyte progenitors<sup>31</sup>, human intestinal epithelia cells<sup>32</sup>, and erythroid progenitors<sup>33</sup>, p27 levels increase just prior to differentiation. Upregulation of p21 in differentiating cells has been observed in differentiation of erythroid progenitors<sup>33</sup>, neuroblastomas<sup>34</sup>, mouse oligodendrocytes<sup>35</sup>, mouse keratinocytes<sup>36</sup>, and human intestinal epithelial cells<sup>32</sup>, with timing of upregulation varying early or late in the differentiation process dependent on the cell type under study. Protein levels of p21 and p27 both increase as hESC differentiate<sup>37</sup>.

Cyclin D1 increases with differentiation of human myeloid leukemia cell lines<sup>38</sup>, hECC lines directed towards neuroectoderm<sup>39</sup>, and in neurite differentiation<sup>40</sup>. Knockdown of Cyclin D1 abolished neurite differentiation, suggesting that Cyclin D1 is critical for some types of differentiation<sup>40</sup>. Overexpression of Cyclin E or Cyclin D1 in Rat-1 fibroblasts shortens G1<sup>41</sup>. Cyclin E overexpression prevents exit from the cell cycle during *Drosophila* embryogenesis<sup>2</sup>.

Through series of complementation studies in pRb <sup>-/-</sup> mice, or conditional knockdowns of pRb, roles for pRb in cellular differentiation in several tissue types have been established. pRb promotes differentiation of skeletal<sup>42</sup> and cardiac muscle<sup>43</sup>, osteoblasts<sup>44</sup>, and thryocytes<sup>45</sup>, but appears to inhibit differentiation of brown adipocytes in both mouse embryonic fibroblasts (MEFs) and mouse embryonic stem cells (mESC)<sup>46</sup>.

#### Expression of G1 regulatory molecules in human embryonic stem cells

The atypical cell cycle profile found in hESC is accompanied by a similarly atypical expression profile of cell cycle molecules that regulate G1. The regulatory molecules that mediate S-G2 transition, and transit through mitosis (Cyclin A and CDK6, and Cyclin B1, respectively) are cell cycle regulated<sup>47</sup>, while the G1 regulatory molecule expression patterns differ from that of somatic cells (see Figure 2).

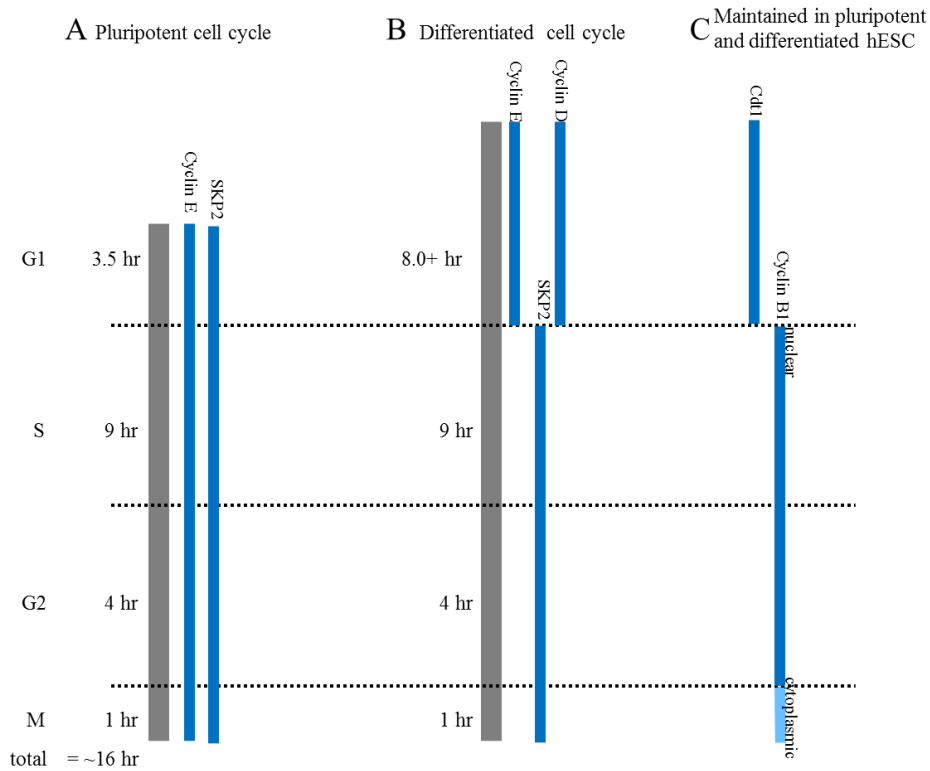


**Figure 2:** Expression profiles of active cell cycle regulators in **A:** human embryonic stem cells compared to **B:** differentiated or somatic human cells. In hESC G1 is truncated, possibly due to a reduction in early G1, while S-phase is elongated compared to differentiated cells. Cyclin E may be continuously expressed during the entire cell cycle in hESC where in differentiated cells is expression is limited to late G1. **C:** Cell cycle molecules with regulation maintained in hESC compared to differentiated cells.

A handful of studies of cell cycle regulation in hESC have been performed, and the varied approaches of these studies make it difficult to compare or extrapolate results from one published account to another. The majority of these studies used bulk cultures of pluripotent or differentiating hESC and examined protein or transcript levels across the population as a whole. While this provides a comprehensive look at the entire population of hESC, these results provide only correlative data of trends of cell cycle marker expression and pluripotent or differentiation markers. Only one study to date has examined hESC cultures on a cellular level, directly quantifying cell cycle marker expression in individual cells measured for presence or absence of pluripotency makers OCT4 or GCTM-2<sup>48</sup>. Given the heterogeneity present in hESC cultures between passages, due to varying amounts of uncontrollable spontaneous differentiation, it is necessary to use caution when interpreting results of data generated from bulk cultures. Greater confidence can be given to results that account for this population variance by directly measuring cell cycle molecule expression in pluripotent versus differentiated cells. Despite the possibility that spontaneously differentiating cells

present in control or “undifferentiated” hESC cultures could skew results, several conserved trends in cell cycle regulation are noticeable in published accounts to date.

Cyclin D1 is expressed at low levels or absent in pluripotent hESC and its expression increases with differentiation. Bulk pluripotent hESC cultures show low Cyclin D1 protein by Western blot and mRNA in both unsynchronized<sup>47,49</sup> and mitotically-released populations<sup>49</sup>. These same studies showed that pluripotent hESC express low levels of Cyclin D1 and that differentiation induces an increase in protein and transcript levels of Cyclin D1. Indirect double immunofluorescence for Cyclin D1 and OCT4 in spontaneously differentiated hESC shows no Cyclin D1 expression in cells positive for OCT4, but OCT4 negative cells stain positive for Cyclin D1<sup>50</sup>. Whether these differences are due to the increased sensitivity of detecting protein by Western blot compared to immunofluorescence or possibly due to contaminating bias by differentiated cells present in the bulk cultures has not been determined. However, it is clear that Cyclin D1 levels increase in hESC with differentiation.

Cyclin E is periodically expressed at both protein and mRNA levels, and is highly expressed in pluripotent hESC. According to Filipczyk *et al* 99% of OCT4-positive cells are also positive for Cyclin E, whereas only 18% of cells OCT4-negative express Cyclin E, as quantified by double indirect immunofluorescence<sup>50</sup>. Given that differentiated hESC typically show approximately 60-70% of cells in G1<sup>47,50</sup>, this estimate of 18% of differentiated cells expressing Cyclin E seems low. It has not been determined whether this population of Cyclin E-positive/OCT4-negative cells is indicative of cells residing in late G1 before transition to S-phase, in keeping with published accounts of Cyclin E activity occurring in late G1 in somatic cell types<sup>41</sup>. A second conflict is apparent within Cyclin E accounts in hESC: Filipczyk *et al* demonstrate nearly all OCT4 positive cells are positive for Cyclin E, but mRNA and protein data from Neganova *et al.* suggests that Cyclin E levels fluctuate throughout the cell cycle of bulk cultured hESC. If Cyclin E levels are phasic, it would not be expected that all pluripotent cells should stain positive for this cell cycle marker, but rather a fraction equivalent to the percent of G1-residing pluripotent hESC, approximately 18-20%<sup>1,47,50</sup>. Again, if the disparity in these results is due to the difference in experimental design is not clear and highlights the importance of corroborating cell identity by pluripotency marker with cell cycle profile.

CDK2 has been implicated as a key cell cycle molecule required for pluripotency. Inhibition of CDK2 by the small molecule Roscovitine induces a two-fold increase in the number of G1-residing cells along with a decrease in cells

positive for OCT4<sup>50</sup>. Phosphorylation of pRb by CDK2 in synchronized hESC was higher than activity of CDK4/6, although the high activity of CDK2 was reported to occur in S-phase<sup>47</sup>. In the same study, knockdown of CDK2 by siRNA induced G1 arrest, loss of pluripotency markers OCT4, SOX2, NANOG, SSEA-3, and an increase in Cyclin D2, p27 and p21, suggested markers of differentiation.

The status of pRb in hESC has not been clearly elucidated. In mESC pRb is constitutively inactivated through hyperphosphorylation<sup>13</sup>, eliminating early G1. These results have traditionally been extrapolated to hESC though until recently there was no evidence of lack of un/hypophosphorylated pRb. Filipczyk *et al* demonstrated the presence of both hypo- and hyper-phosphorylated pRb within the fraction of hESC positive for pluripotency marker GCTM-2, and that the hypophosphorylated form increases with differentiation<sup>50</sup>. These results suggest that there is a functioning R-point within hESC and an early G1 phase is present. How pRb may be hyperphosphorylated in hESC in the absence of Cyclin D1 has not been established in light of evidence demonstrating that Cyclin D1 activity is rate-limiting for S-phase entry<sup>41</sup>. Early work in characterizing the role of Cyclins D1 and E demonstrated that expression of Cyclin E alone in the absence of Cyclin D1 did not produce transit through G1<sup>41</sup>. Future work in this area may yield interesting results regarding unique mechanisms of R-point passage in hESC.

To date, two novel intersections between mechanisms of pluripotency and cell cycle regulation have been established in hESC. NANOG, a master regulator of pluripotency, has been shown to regulate transcription of CDK6 to induce quickened G1-S transit<sup>51</sup>. Cyclin D1 levels are kept low in pluripotent hESC through post-transcriptional degradation by miR-302, which is controlled by both OCT4 and NANOG<sup>52</sup>. miR-302 is specifically expressed in hESC and hECC<sup>53</sup> and is downregulated with differentiation. Expression of miR-302 in somatic cells induces a hESC-like cell cycle distribution<sup>52</sup>.

A strong linkage can be found within the current literature between cell cycle changes and development. Changes in cell cycle phase profiles occur in coordination with embryonic development<sup>10,12,54,55</sup>. Differentiation of pluripotent and multipotent cells leads to lengthened cell cycle by virtue of G1 phase extensions<sup>20,56</sup>, with the corollary that pathways that regulate pluripotency of hESC establish truncated cell cycle parameters<sup>53,57</sup>. Despite these clear trends, the actual details of G1 phase changes during the differentiation of pluripotent cells has yet to be clearly demonstrated. In addition, the kinetics of cell cycle changes such as G1-extension onset remain unanswered during lineage-specific differentiation of hESC. We have used live-cell and high content imaging of a fluorescent cell cycle reporter to address these questions during the

differentiation of hESCs in response to chemical compounds and protocols directing mesoderm, endoderm or ectoderm.

#### Live fluorescent cell cycle reporter

In 2008, Sakaue-Sawano and colleagues published the first demonstration of the live fluorescent cell cycle reporter they termed Fucci Orange<sup>58</sup>. Fucci Orange is a fusion of an orange fluorophore, mKO2<sup>59</sup>, to a truncated fragment of the DNA licensing protein, Cdt1 (Figure 4). Fucci Orange reporter destruction is regulated by one of the three mechanisms regulating full length Cdt1. The Fucci Orange Cdt1 truncation retains a Cy-motif at residues 68-70 that is phosphorylated by Cyclin E-CDK4 and Cyclin A-CDK2, marking the protein for ubiquitylation by the E3 ligase component of SCF<sup>Skp2</sup><sup>60,61</sup>. Fucci Orange does not contain any elements involved in DNA licensing, ensuring that DNA replication remains normal in transgenic lines. The authors of the original report created transgenic mice and cell lines carrying the Fucci Orange reporter; these mice appeared developmentally normal, suggesting that expression of the Fucci Orange reporter does not disturb critical developmental and biological processes.

Human Cdt1 degradation is regulated by two distinct mechanisms in addition to the SCF<sup>Skp2</sup>-dependent polyubiquitination pathway described above. A second polyubiquitin-mediated proteolysis pathway targets Cdt1 for destruction by the E3 ligase Cdt2<sup>62</sup>, as part of the CLR4<sup>Cdt2</sup> complex. Both Cdt1 and Cdt2 contain PIP-box motifs to associate with chromatin-bound PCNA<sup>63,64</sup>. Cdt1 associates with PCNA through its N-terminus PIP-box sequence at residues 3-10. After DNA replication has been initiated, PCNA-bound Cdt1 is polyubiquitinated by PCNA-bound Cdt2<sup>61,65</sup>. PIP-box mediated PCNA binding is required for S-phase Cdt1 degradation during DNA replication<sup>65,66</sup> and is required for normal cell division without inappropriate DNA re-replication<sup>67</sup>. This mechanism also operates after DNA damage by UV irradiation<sup>61,68</sup>. Following DNA damage, Cdt1 is recruited to damage sites by its PIP-box and quickly degraded in a PCNA- and Cdt2-dependent manner<sup>68,69</sup>. Cdt1 is required for break induced repair of DNA<sup>70</sup>. Cdt1 is inhibited by Geminin binding, due to blocking of critical residues required for Cdt1 to bind to DNA<sup>71</sup>. Thus, Geminin-bound Cdt1 cannot participate in pre-RC formation and DNA cannot be replicated.

#### Differentiation of human embryonic stem cells

In this study we used small molecules to initiate differentiation of hESC, and the properties of these molecules are discussed below.

### *RRD-251*

Raf-1 phosphorylates pRb in early G1 in response to mitogen stimulation<sup>72</sup>. Raf-1 mediated phosphorylation is thought to be the initial event in the series of inactivating phosphorylations of pRb, ultimately leading to release of E2F-family transcription factors that permit transition to S-phase from G1. Inhibition of Raf-1/pRb interaction results in failure of E2F-dependent transcription and causes G1-arrest. RRD-251 is a small molecule disruptor of the Raf-1/pRb interaction<sup>73</sup>. Treatment with RRD-251 induces cell cycle arrest and apoptosis, reduces tumour size, and inhibits angiogenesis when tested on small cell lung carcinoma and human melanoma cell lines and xenografts<sup>73,74</sup>.

### *DMSO*

Dimethyl sulfoxide (DMSO) was originally discovered as an inducer of terminal differentiation in Friend murine leukemia cells during toxicity dose trials<sup>75</sup>. DMSO-treated murine erythroleukemic (MEL) cells show a change in alkaline sucrose gradient sedimentation rate, suggesting a change in DNA structure occurs along with the differentiation process<sup>76</sup>. DNA fragmentation or weakened association of DNA with chromosome structure facilitating strand denaturation in alkaline conditions were offered as possible explanation for the DMSO-induced change in sedimentation rate. Initial experiments suggesting DMSO-induced differentiation is accompanied by DNA damage<sup>76</sup> were later repudiated by evidence suggesting that DNA fragments may result from initiation of mRNA synthesis<sup>77</sup>. A number of chromatin conformational changes are induced by DMSO that can be explained by hyperacetylation of chromatin<sup>78,79</sup>. Lengthening of G1 phase with differentiation has been observed for MEL cells treated with DMSO<sup>80</sup>. DMSO is a histone deacetylase inhibitor<sup>81</sup>, and induces hyperacetylation of histones. Hyperacetylation of chromatin induces increased gene expression by permitting access to transcriptional start sites by DNA transcriptional machinery<sup>82,83</sup>. Chromatin hyperacetylation is associated with differentiation status of hESC<sup>84</sup>. DMSO is known to cause differentiation of hESC.<sup>85</sup>

### *HMBA*

After the observation that DMSO was capable of inducing differentiation in Friend MEL cells, other compounds were investigated for the potential of increased efficiency at inducing differentiation compared to DMSO. Hexamethylene bisacetamide (HMBA) was synthesized in a series of polymethylene bisacetamides containing between two and eight methylene

groups. HMBA is a potent inducer of MEL differentiation at concentrations well below that used for DMSO<sup>86</sup>. HMBA-induced differentiation of MEL cells leads to G1 arrest, suppresses CDK4, and increases levels of p27. G1 phase extension requires exposure to HMBA during the G1 phase of the cell cycle prior to the prolonged phase<sup>87,88</sup>. Expression of differentiation genes is also detected during the G1 phase of the second cell cycle following exposure to HMBA<sup>87</sup>. Differentiation induced by HMBA treatment produces accumulation of unphosphorylated pRb, decrease in Cyclin A levels, increase in p27 levels, suppression of Cyclin E-CDK2 activity, and increased susceptibility to apoptosis<sup>88-93</sup>. HMBA has been used to differentiate a variety of cell types, including MEL, T-ALL, T24, hECC, and hESC<sup>85,87,90,92-94</sup>. Phase I and II trials to test efficacy and safety of HMBA as a chemotherapeutic agent appeared promising, but the compound could not be used clinically due to significant side effects and the high concentration of drug needed to induce remission in patients<sup>95,96</sup>. HMBA is known to cause differentiation of hESC.<sup>85</sup>

#### *Retinoic acid*

Retinoic acid (RA) is a small molecule derivative of Vitamin A, and is endogenously expressed within the developing vertebrate embryo. RA is critical to proper anterior-posterior patterning during development through regulation of HOX gene expression. RA binds to the retinoic acid receptor (RAR), a type II nuclear receptor bound to DNA. RARs bind to DNA sequences termed retinoic acid response elements (RARE) located close to RA-responsive genes. Upon binding of RA to a RAR, RAR-bound co-repressors dissociate and co-activators are recruited to the site, resulting in activation of nearby RA-responsive genes. Addition of exogenous RA to embryos can alter body patterning, including truncation of structures or respecification of anterior structures to posterior locations<sup>97</sup>.

Retinoic acid has been used to differentiate hECC, hESC, and human leukemia line HL-60. Differentiation of embryonal carcinoma cells was cell-cycle dependent and increased cell cycle length, due to an extension of G1 phase length<sup>98-100</sup>. HL-60 cells are sensitive to differentiation by exposure of RA during G1, but not other phases of the cell cycle<sup>101</sup>. Expression of neural lineage-related markers is increased with differentiation by RA<sup>85,102</sup>, and may occur by inhibition of proteasome-dependent degradation of the G1-phase CKI p27<sup>103</sup>. Retinoic acid neural induction of hECC and hESC is cell density-dependent<sup>104</sup>. Human embryonal carcinoma cell differentiation with retinoic acid induces HOX gene expression in response to varying concentrations of RA, dependent on the location

of the target gene within a specific locus<sup>105</sup>. In keeping with observations from vertebrate embryonic development, genes at the 3' end respond to a lower concentration of RA, while genes at the 5' end require concentrations of retinoic acid 2 to three orders of magnitude higher. At the highest concentration of RA used, 10<sup>-5</sup> M RA, all HOX genes studied were activated sequentially in a 3' to 5' direction.

#### *LY294002*

LY294002 is a small molecule inhibitor of phosphatidylinositol 3-kinase (PI3K)<sup>106</sup>. PI3K enzymes are activated by growth factors and hormones to phosphorylate lipids and proteins, initiating pathways to drive cell growth, cell cycle entry, cell migration, and cell survival<sup>107</sup>. Phosphorylation of PI3K target lipids recruits signalling molecules to the plasma membrane, where they in turn are phosphorylated. PI3K targets include protein serine-threonine kinases, protein tyrosine kinases, and G-proteins. Once phosphorylated, PI3K target proteins initiate signalling cascades.

Akt is activated by phosphorylation following growth factor activation of PI3K. Activated Akt initiates signalling cascades, resulting in activation of molecules necessary for cell cycle entry and cell survival. For example, Akt phosphorylates proteins required for apoptosis, resulting in blockage of this cell death pathway promoting cell survival<sup>108</sup>. Akt activation initiates a cascade initiating p27 transcription<sup>109</sup>. PI3K and Akt activity support pluripotency of hESC<sup>110-113</sup>.

#### Human embryonic stem cells and screening

High-throughput (HTS) and high-content (HCS) screening are valuable methods for fast, reproducible assay of small molecules and proteins to find biologically active compounds. hESC or other pluripotent cell types would be useful screening candidates given their species and developmental relevance. Screening large libraries of compounds on hESC could reveal useful compounds maintaining self-renewal, or directing differentiation towards specific lineages. The results of such screens could help direct lineage-specific derivation of cell types used in replacement or regenerative therapies, or reveal new molecules that may be helpful to stem cell biology research.

Most HTS or HCS efforts using hESC use single-cell dissociation to plate equal numbers of cells in small well format plates and require thorough examination of the best way to adapt hESC to useable screening formats<sup>114</sup>. hESC are extremely sensitive to single cell dissociation<sup>115</sup>, with few cells surviving the

treatment. These screens have primarily revealed small molecules that increase hESC survival under these harsh conditions, based on quantitative analysis of OCT4 indirect immunofluorescence end-point assays<sup>116-118</sup>. RNAi<sup>119,120</sup>, proteome<sup>121</sup>, and transcriptome<sup>122</sup> screens of hESC have each revealed genes important for maintenance of hESC self-renewal and pluripotency. hESC have also been used to demonstrate quantitative screening as a tool for finding factors required for endoderm formation<sup>123</sup>. Screens targeting molecules to direct lineage specific cell types or targets have used hESC-derived precursor cell types, rather than pluripotent hESC populations<sup>124,125</sup>. Our study has used hESC in conjunction with HCS to develop novel techniques and technologies that are complementary to eventual utilization of our reporters in HTS scenarios.

## Methods

### Cell culture

H1, and H9 hESC lines<sup>126</sup> were cultured on x-ray inactivated MEFs on 1.0% gelatin-coated tissue culture plates (Falcon). Cells were passaged when nearly confluent, approximately every 5 to 7 days. Briefly, cells were treated with 1mg/ml Collagenase IV (Invitrogen) at 37°C until colony edges show peeling, mechanically scraped, spun down, and replated at 1:6. hESC were maintained in KO DMEM (Invitrogen), with 15% serum replacement (Invitrogen), 2 mM Gluta-Max (Invitrogen), 100 uM non-essential amino acids (Invitrogen), 8ng/ml bFGF (Peprotech).

### Generation of reporter constructs

The Fucci Orange reporter sequence (MBL) was cloned into expression vectors under the control of a CAG promoter for expression in hESC. Two variants were created: *pCAG CAG-mKO2 Cdt1 IRES Puro* (Fucci), and *pCAG H2B GFP F2A mKO2 Cdt1 IRES Puro* (CAG-H2GFOIP). *pCAG H2GFOIP* was created by ligating a H2GFOIP insert (AvrII (blunt)/BglII digested) into a *pCAG* expression vector (Age (blunt)/BglIII digested). Colonies were screened by diagnostic PCR with a BglII-H2B forward primer and GFP-Nhe reverse primer. Positive colonies were cultured; plasmid DNA isolated (Qigen mini prep kit) and digested with Kpn for; confirmation of proper cassette orientation in the *pCAG* expression vector; and sequenced to confirm the absence of mutations (MOBIX, McMaster University). All restriction enzymes were by Fermentas. Each expression cassette was additionally cloned into a PiggyBac transposable vector (*pB CAG-mKO2 Cdt1 IRES Puro*, and *pB H2B GFP F2A mKO2 Cdt1 IRES Puro*). PiggyBac expression vectors were a gift from the Nagy lab (Mount Sinai Hospital, Toronto ON).

### Generation of stable reporter hESC lines

20 ug of linearized *pCAG CAG-mKO2 Cdt1 IRES Puro*, and *pCAG H2B GFP F2A mKO2 Cdt1 IRES Puro* expression plasmids were electroporated into H1<sup>126</sup> and H9 (WiCell) hESC parental lines. PiggyBac H1 and H9 hESC lines were created with 20 µg of *pB CAG CAG-H2GFOIP* plus 5 µg of transposase *pCYL43* (Sanger Institute, UK). Electroporation conditions were based on those previously described<sup>127</sup>. Cells were selected with Puromycin (1 µg/mL) for two days, permitted to recover, and individual colonies picked manually once established.

Clones used in this work: H1 *pCAG H2B GFP F2A mKO2 Cdt1 IRES Puro* 13 (H1-13 CAG-H2GFOIP); H1 *pCAG CAG-mKO2 Cdt1 IRES Puro* B3 (H1 Fucci B3); H9 *pCAG CAG-mKO2 Cdt1 IRES Puro* D4 (H9 Fucci D4); and H9 *pB H2B GFP F2A mKO2 Cdt1 IRES Puro* 12 (H9 CAG-H2GFOIP 12).

#### Time lapse imaging

CAG-H2GFOIP cells were passaged and plated as described above. Two days after passage once nascent colonies were visible hESC media was changed for differentiation media (defined below). Plates were immediately placed in a Nikon BioStation CT for observation. Colonies were visually selected for time lapse observation by phenotypic appearance typical of pluripotent hESC. Three colonies per well, with two wells per treatment, were observed every 6 hours for dose curve experiments. High resolution time points were acquired every 15 minutes on three colonies per well, with one well per treatment using CAG-H2GFOIP.

#### Differentiation

Chemicals and small molecule inducers of differentiation were diluted in complete hESC media (defined above). Compounds and final concentrations used were: 1.0% DMSO (Sigma-Aldrich); 3 mM HMBA (Sigma-Aldrich); 40 uM RRD-251 (Sigma-Aldrich); 40 uM LY294002 (Calbiochem); 10<sup>-5</sup>M retinoic acid (Sigma-Aldrich).

Endoderm derivation protocols were based on those previously described.<sup>128</sup> hESC are grown to near confluence, then washed 1x with PBS and placed in basal endoderm differentiation media RPMI (Sigma-Aldrich) with 2 mM Gluta-Max supplemented each day as follows:

Day 1	100 ng/mL Activin A (Peprotech) 25 ng/mL Wnt3a
Day 2, 3	100 ng/mL Activin A 0.2% FBS (Hyclone)
Day 4, 5	100 ng/mL Activin A 2.0% FBS (Hyclone)

Cells were fixed as described here after day 5 of endoderm induction.

Neural differentiation was based on a previously described protocol<sup>129</sup>. Monolayer hESC were cultured to approximately 60% confluency, and then hESC media without bFGF supplemented with 5uM SB431542 (Tocris) and 5uM Dorsomorphin (Tocris) was added to cells. Media was changed every two days.

Cells were then grown in DMEM-F12 (Invitrogen) with 1x N2 supplement (Invitrogen) and 20ng/ml bFGF for 6 days. Media was changed every 2 days.

Mesoderm differentiation was adapted from haematopoietic differentiation protocols previously used.<sup>130</sup> After monolayer hESC had reached 60% confluency, they were cultured in serum-free DMEM-F12 supplemented with 300 ng/ml stem cell factor (SCF; Amgen), 50 ng/ml granulocyte colony stimulating factor (G-CSF; Amgen), 25 ng/ml bone morphogenic protein-4 (BMP-4; R&D systems), 10 ng/ml interleukin-3 (IL-3; R&D systems), 10 ng/ml interleukin-6 (IL-6; R&D systems), and 300 ng/ml Flt-3 ligand (Flt-3 L: R&D systems) for five days.

#### Flow cytometry

H1-13 CAG-H2GFOIP cells were differentiated for 48 hours and stained for cell surface markers. Briefly, following differentiation, cells were washed once with 1x PBS, and singularized with TrypLE (Invitrogen) with gentle titration after five minutes incubation at 37°C. Cells were washed and collected in hESC media, and pelleted at 1200 rpm for 3 minutes, then resuspended in flow cytometry buffer (1x PBS with 1% FBS and 1 mM EDTA) and filtered through a 35 µm mesh-topped flow cytometry tube (Falcon) to remove debris and cellular aggregates. Staining was performed on ice for 20 minutes in staining buffer (1X PBS with 3% FBS). Antibodies used were conjugated Tra-1-60 APC (BD Pharm 560122 at 1:2000) and SSEA-3. Stained cells were washed twice with flow cytometry buffer and assayed on a BD FACS Calibur. The Fucci Orange fluorophore mKO2 was excited by a 488 nm laser and emission collected by a 585/42 filter; H2B GFP was excited and collected by a 488 nm laser and a 530/30 filter; and APC conjugated antibodies excited and collected with a 635 nm laser and 661/16 filter, respectively. Quantification and analysis of results were performed on FlowJo (Treestar).

#### FACS

Cell sorting was performed on a BD FACS Aria II (BD Biosciences). Cells were prepared as described above. H2B GFP and mKO2 were excited and collected by 488 nm laser and 530/30 filter, and 488 nm laser and 585/42 filter, respectively.

#### Indirect immunofluorescence

Fucci Orange hESC were passaged and differentiated as described here. Cells were washed once with 1x PBS with  $Mg^{+2}/Ca^{+2}$ , fixed at room temperature for 8 minutes with 4% PFA in 1x PBS with  $Mg^{+2}/Ca^{+2}$ , and washed three times with 1x

PBS. Fixed cells were permeabilized with ice-cold 100% methanol for two minutes at room temperature and washed three more time with PBS. Before staining cells were blocked for 15 minutes at room temperature with 1% BSA (Sigma-Aldrich) in 1x PBS and washed once with 1x PBS. Antibodies were diluted in blocking solution. Primary antibodies were incubated at 4°C overnight, washed three times with 1x PBS, and secondary antibodies incubated for 1 hr at room temperature. Stained cells were stored in 1x PBS with Hoechst 33342 nuclear stain. Antibodies used were as follows: OCT4 (BD 611203) at 1:200 with goat anti-mouse AF 647 (Invitrogen A-21238); EOMES (Abcam AB23345) at 1:50 with donkey anti-rabbit AF647 (Invitrogen A-31571); GATA4 (Santa Cruz sc-9053) at 1:200 with donkey anti-rabbit AF647; TCF2 (BD 612504) at 1:250 with goat anti-mouse AF647; SKP2 (Cell Signalling 4358) at 1:50 with goat anti-rabbit AF 488 (Invitrogen A-11070); and Cyclin B1 (Cell Signalling 4138) with goat anti-rabbit AF 488. All secondary antibodies were used at 1:500 dilution. Cyclin B1 stained cells were imaged on an Olympus IX51 microscope on 20x magnification. All other imaging was performed a Cellomics ArrayScan HCS Reader (Thermo Scientific). ArrayScan images were taken as a seamless montage of 16 individual tiles comprising approximately 0.24 cm<sup>2</sup> surface area of each well.

#### Image analysis

Image analysis of immunofluorescence and reporter fluorescence acquired with the ArrayScan was performed in Accapella and quantification in MatLab, with custom scripts written for both programs by Dr. Tony Collins. Using Accapella scripts, cells were identified by Hoechst 33342 staining intensity. Each Hoechst 33342-positive object was then read for fluorescence intensity across multiple channels for Fucci Orange reporter, and secondary antibody staining levels. Values recorded represent pixel intensity of acquired images. In MatLab, fluorescence intensity values per object were displayed in a two dimensional plot, to quantify co-expression of any two selected fluorescence channels. Positive objects for each channel were determined by visual identification of positive nuclei in Accapella. The recorded fluorescence intensity values determined by Accapella were applied as threshold settings for quantification outputs in MatLab. Image analysis work flow is represented below in Figure 3.

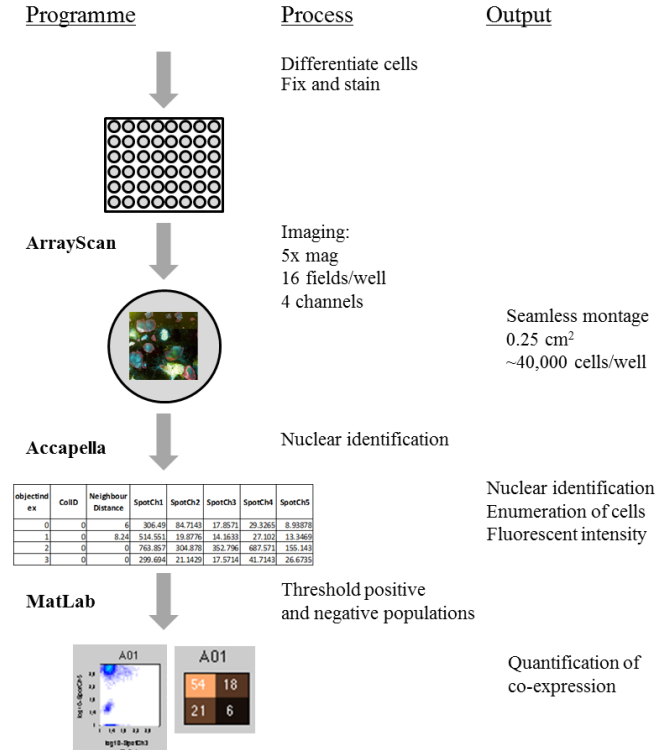


**Figure 3: Image analysis workflow.** Fucci Orange expressing hESC are fixed in 48 well plates and stained with antibodies against proteins of interest. Fixed and stained cells are imaged in the ArrayScan; immunofluorescence images are analyzed in Accapella to identify nuclear objects and record fluorescence for each channel; identified nuclear objects are plotted and thresholds applied in MatLab to quantify co-expression of fluorophore sets.

### RT-qPCR

RT-qPCR was performed on sorted populations of Fucci Orange-positive and –negative cells. Approximately 500,000 cells per population for each experiment were collected. mRNA was extracted (RNAeasy kit, Qiagen), and synthesized to cDNA (iScript kit, Bio-Rad). RT-qPCR reactions were run with SYBR Green (Bio-Rad) on a CFX96 Touch™ Real-Time PCR Detection System (Bio-Rad). Analysis was performed with Bio-Rad CFX Manager software.

### Colony initiating cell assay

H9 Fucci Orange 12 cells were grown in standard hESC media until confluent, and sorted into Fucci Orange-positive and Fucci Orange-negative populations as described above. Isolated populations of cells were plated at densities of 25, 50, and 100 thousand cells per well of a six well plate. Three wells per plating density were used. A second replicate of 50 thousand cells were grown with Roc kinase inhibitor Y27632 added to the media for 24 hours following plating to increase cellular viability<sup>115</sup>. Cells were grown for 12 days until established colonies appeared, then fixed and stained for cell surface protein alkaline phosphatase (AP)

activity with a VECTOR Red Alkaline Phosphatase Substrate Kit (Vector laboratories # SK-5100). Plates of fixed and stained cells were scanned on a flatbed scanner (Canon), and image analysis performed in ImageJ ([rsbweb.nih.gov/ij/](http://rsbweb.nih.gov/ij/)) to identify colony units. Total number of colonies per well were automatically quantified in ImageJ using custom scripts.

## Results

### Generation of human embryonic stem cell lines stably expressing a cell cycle reporter

To study the relationship between cell cycle, specifically the length of G1, and differentiation of hESC, we employed a previously established cell cycle reporter, Fucci Orange<sup>58</sup>. Fucci Orange is a G1-indicating live fluorescent reporter created by fusing the fluorophore mKO2<sup>59</sup> to an N-terminus fragment of Cdt1 (CAG-mKO2-Cdt1)<sup>58</sup> (Figure 4A). Truncated Cdt1 in this fusion protein contains only the regulatory elements responsible for its degradation and lacks DNA licensing capabilities. Tight, cell cycle dependent degradation of Cdt1 results in orange fluorescence only during the G1 phase.

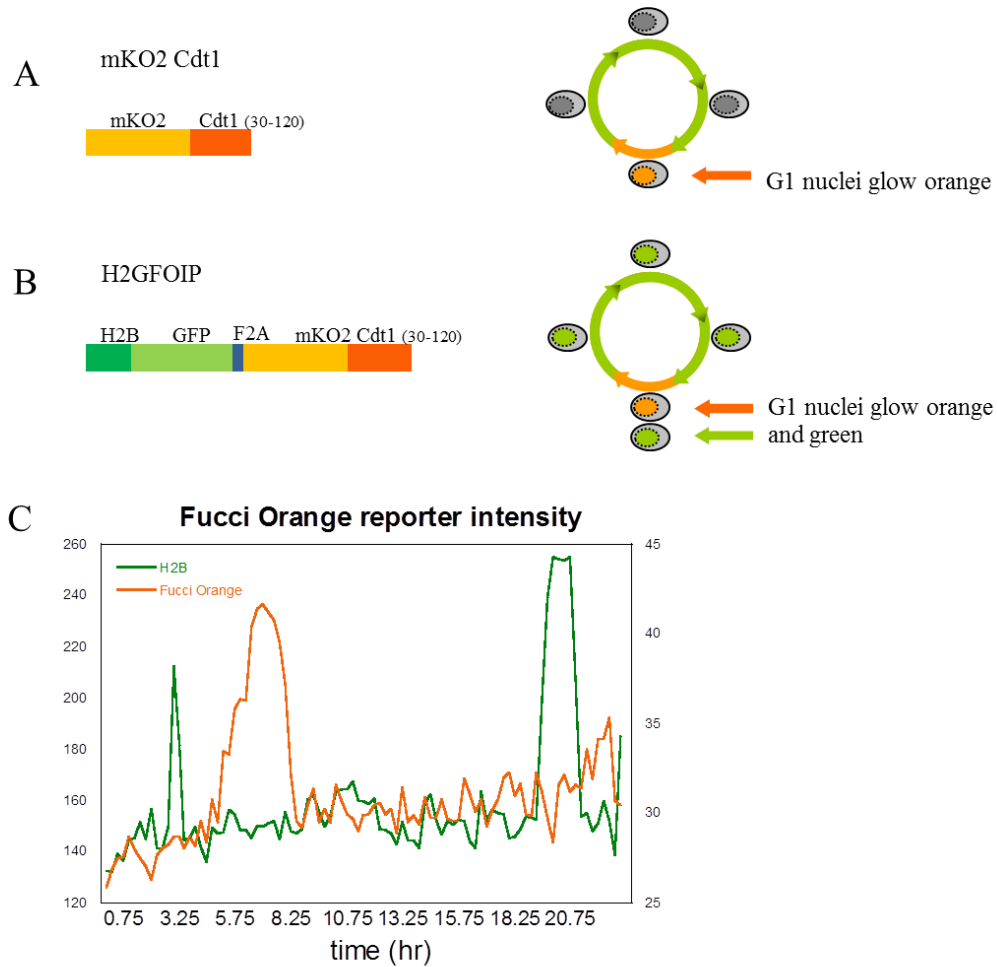


**Figure 4 : Fucci Orange reporter constructs and expression pattern.** **A**, mKO2 Cdt1 fusion marks nuclei of cells residing in G1 phase. **B**, H2GFOIP reporter marks G1 nuclei and all phases are marked by H2B GFP expression. **C**, Intensity of reporter fluorescence in control undifferentiated hESC between mitoses captured during time-lapse imaging.

Fusion of GFP to the histone binding protein H2B effectively demarcates nuclei<sup>131</sup>. We created a dual expression cassette of Fucci Orange complexed with a H2B GFP fusion, H2B-GFP F2A mKO2-Cdt1 (CAG-H2GFOIP, Figure 4B). Use of this dual reporter permits quantification of total cell number within a colony in addition to indicating the G1 status of individual cells. A single powerful promoter, CAG<sup>132</sup>, drives expression of both H2B-GFP and mKO2-Cdt1 fusion proteins, ensuring equal and constant expression of each reporter. F2A is a non-coding linking sequence, post-translationally “cleaved” to yield the two independent proteins<sup>133</sup>. Stable clones expressing each of these reporters have been generated in both H1 and H9 hESC lines and have been used to generate this body of work.

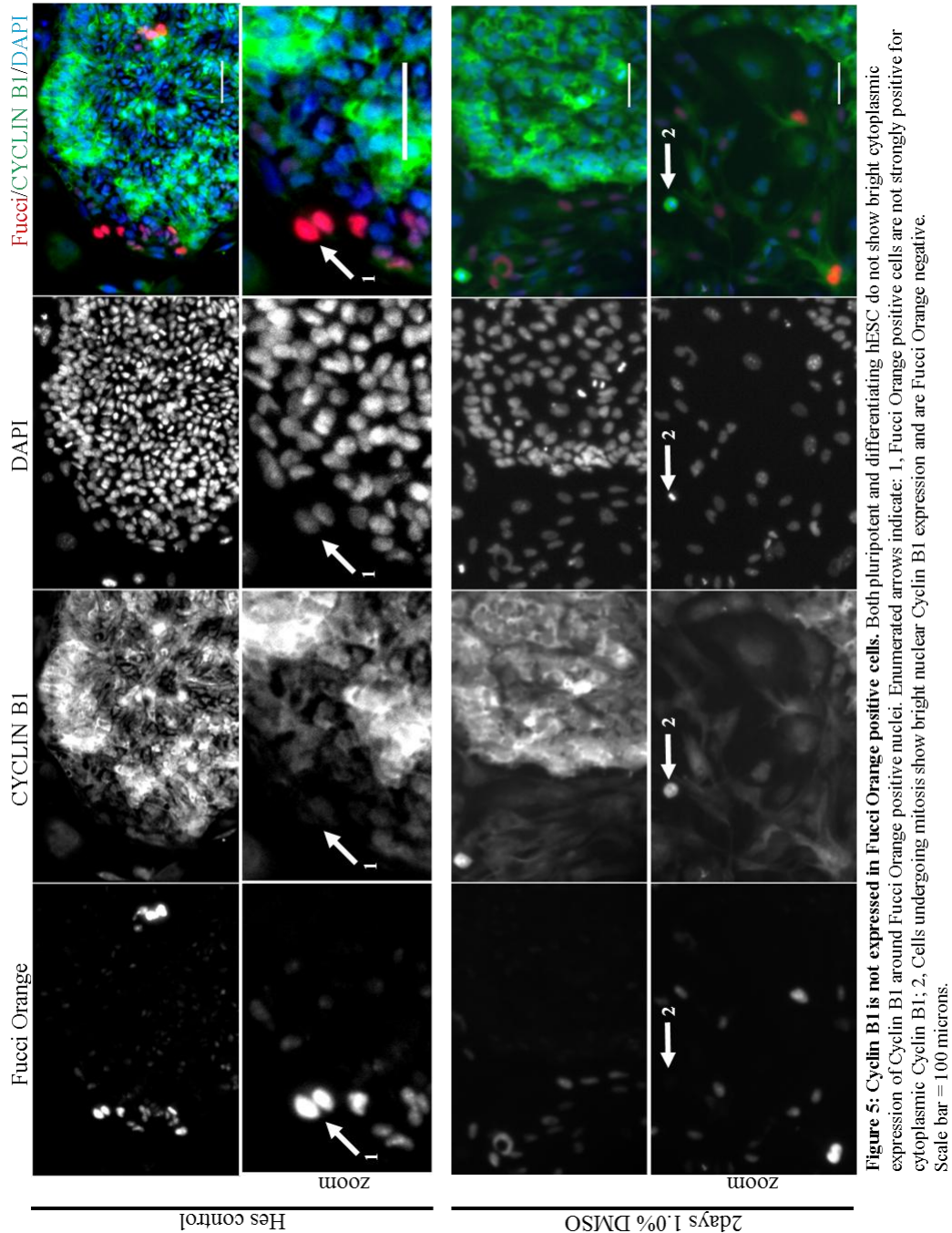
Initial observation of Fucci Orange reporter lines under a fluorescence based microscope indicated periodic expression of the G1 cell cycle reporter within the colonies in contrast to the H2B-GFP that showed ubiquitous expression by visual inspection in the H2GFOIP cell lines. Fucci Orange reporter expression was transient, appeared in only a fraction of cells, and was only weakly fluorescent in colonies appearing morphologically undifferentiated. Numerous large, bright, Fucci Orange nuclei appeared outside of the colony or in masses which appeared to be spontaneously differentiated hESC. These observations were consistent between passages and cell lines. Single cell tracking of high resolution time-lapse imaging experiments showed peak Fucci Orange fluorescence occurring immediately following mitosis (Figure 4C). Mitotic events are detected by peaks in H2B GFP fluorescence intensity, due to compaction of daughter nuclei undergoing segregation. Mitoses of a single tracked cell give a cell cycle time estimate of approximately 17 hours, and duration of Fucci Orange fluorescence estimates a G1 phase lasting about 3.5 hours in undifferentiated hESC (Figure 4C). These values are in agreement with other published accounts.<sup>1</sup> We next used these cell lines to investigate relationships between cell cycle and differentiation under a variety of conditions.

#### Validation of G1-exclusive expression of Fucci Orange reporter

We first validated the expression of the Fucci Orange reporter, by comparing Fucci Orange expression patterns to that of known cell cycle markers of mitosis, S and G2 phases.

Localization of Cyclin B1 varies throughout the cell cycle; it is cytoplasmic from S phase through late G2, then nuclear during mitosis, and degraded during G1<sup>134</sup>. This localization pattern is thought to be maintained in both pluripotent and differentiating hESC.<sup>1,135,136</sup> We therefore attempted to use

Cyclin B1 staining to validate cell cycle specific periodicity of the Fucci Orange reporter. As expected, Fucci Orange-positive nuclei are negative for brightly cytoplasmic Cyclin B1 expression (Figure 5, arrow 1), suggesting that Fucci Orange is restricted to G1. Hoechst nuclear staining can be used to identify cells undergoing mitosis, and these cells are positive for strong nuclear Cyclin B1 expression, and negative for Fucci Orange expression (Figure 5, arrow 2). Together, these data suggest that Fucci Orange-positive cells are not in S, G2 or M phases of the cell cycle.



SKP2 is the E3 ligase component of the SCF<sup>Skp2</sup> complex that is responsible for polyubiquitination of proteins targeted for proteasome-based degradation. SKP2 expression is typically restricted to S through M phases in somatic cells, but it is thought that expression is maintained during G1 in pluripotent hESC, and levels decrease in bulk culture with induction of differentiation<sup>37</sup>. 80% of Fucci Orange-positive cells are negative for SKP2

expression by antibody staining, and 20% of the Fucci Orange-positive population co-expresses Fucci Orange and SKP2 (Figure 6A, Figure 7).

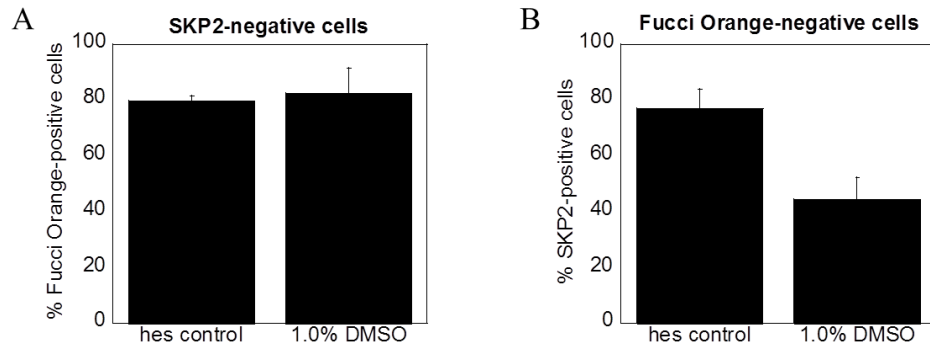


**Figure 6: Fucci Orange and SKP2 are co-expressed in a subset of hESC.** **A:** In both control and 1.0%DMSO-treated cells (48 hours) approximately 20% of hESC are double positive for Fucci Orange and Skp2 expression. **B:** Within the SKP2 positive fraction, a decrease in the number of Fucci Orange negative cells is observed, between the control and DMSO-treated populations. In all plots, bars represent data collected from multiple wells, approximately 80,000 cells per treatment.

The co-expression of the Fucci Orange reporter and SKP2 may be due to SKP2 presence in G1-residing pluripotent hESC. We estimate approximately 20% of the pluripotent hESC population reside in G1, given a total cell cycle time of 17 hours and a G1 length of 3.5 hours (Figure 4C)<sup>1,137</sup>. To address the possibility that the SKP2 protein is constitutively expressed within hESC, we examined the SKP2-positive fraction of hESC and correlated with Fucci Orange expression (Figure 6B). Within the fraction of SKP2-positive cells, the percentage of Fucci Orange-negative cells appears to decrease with DMSO-induced differentiation, suggesting that the SKP2 expression may be maintained in pluripotent hESC. If hESC express SKP2 across all cell cycle phases including G1, and DMSO-differentiation increases the length of G1 and restores cell cycle restriction of

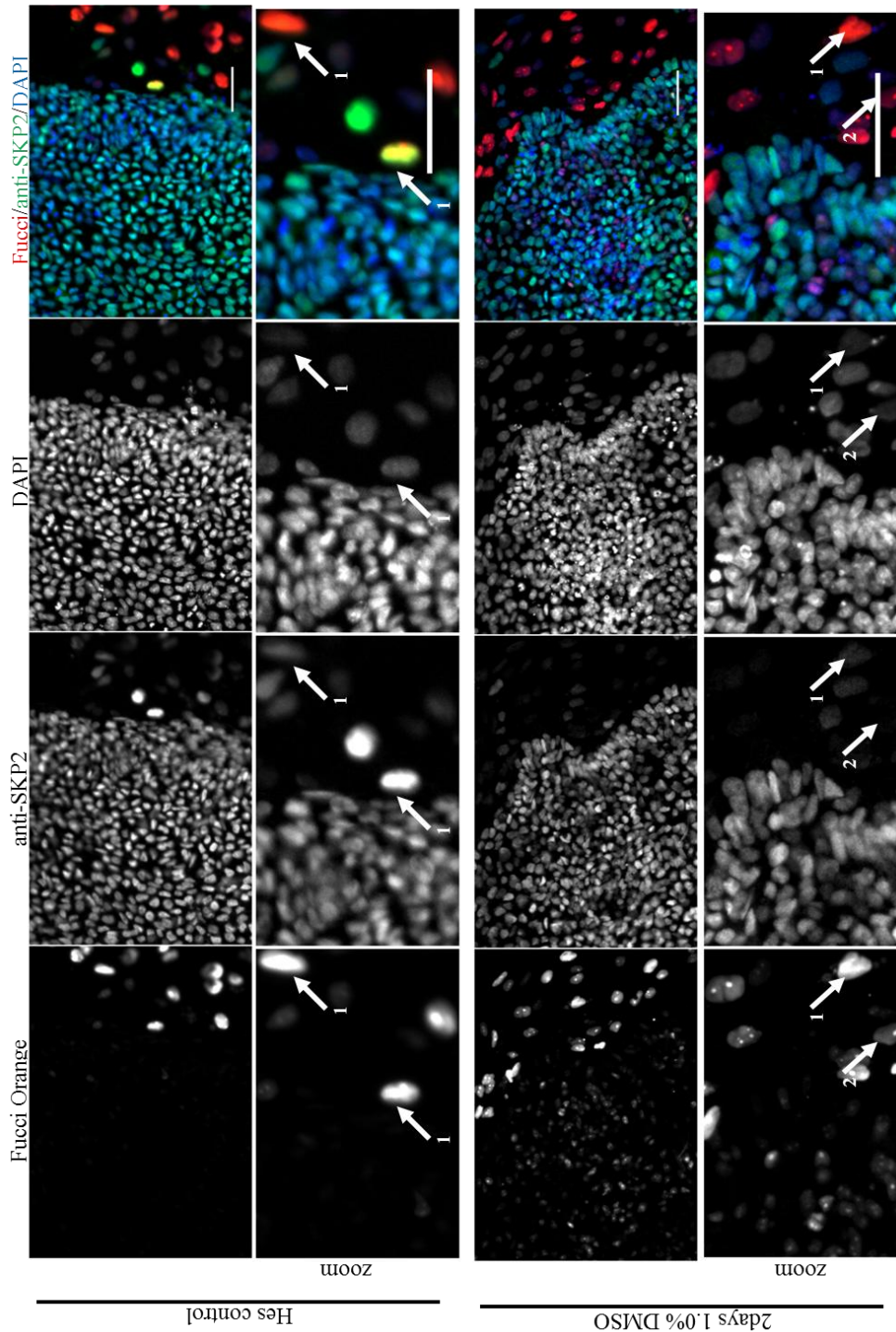
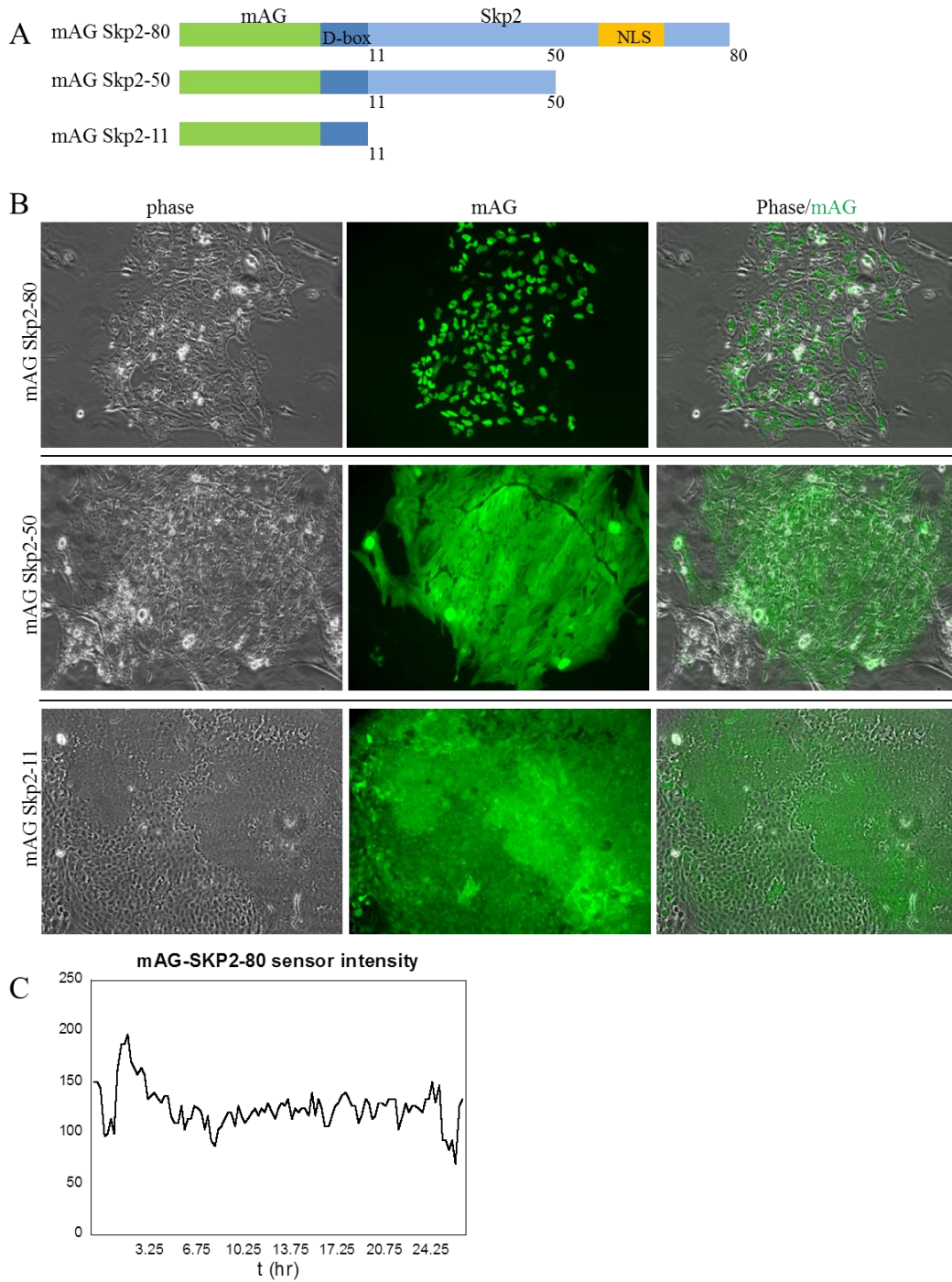


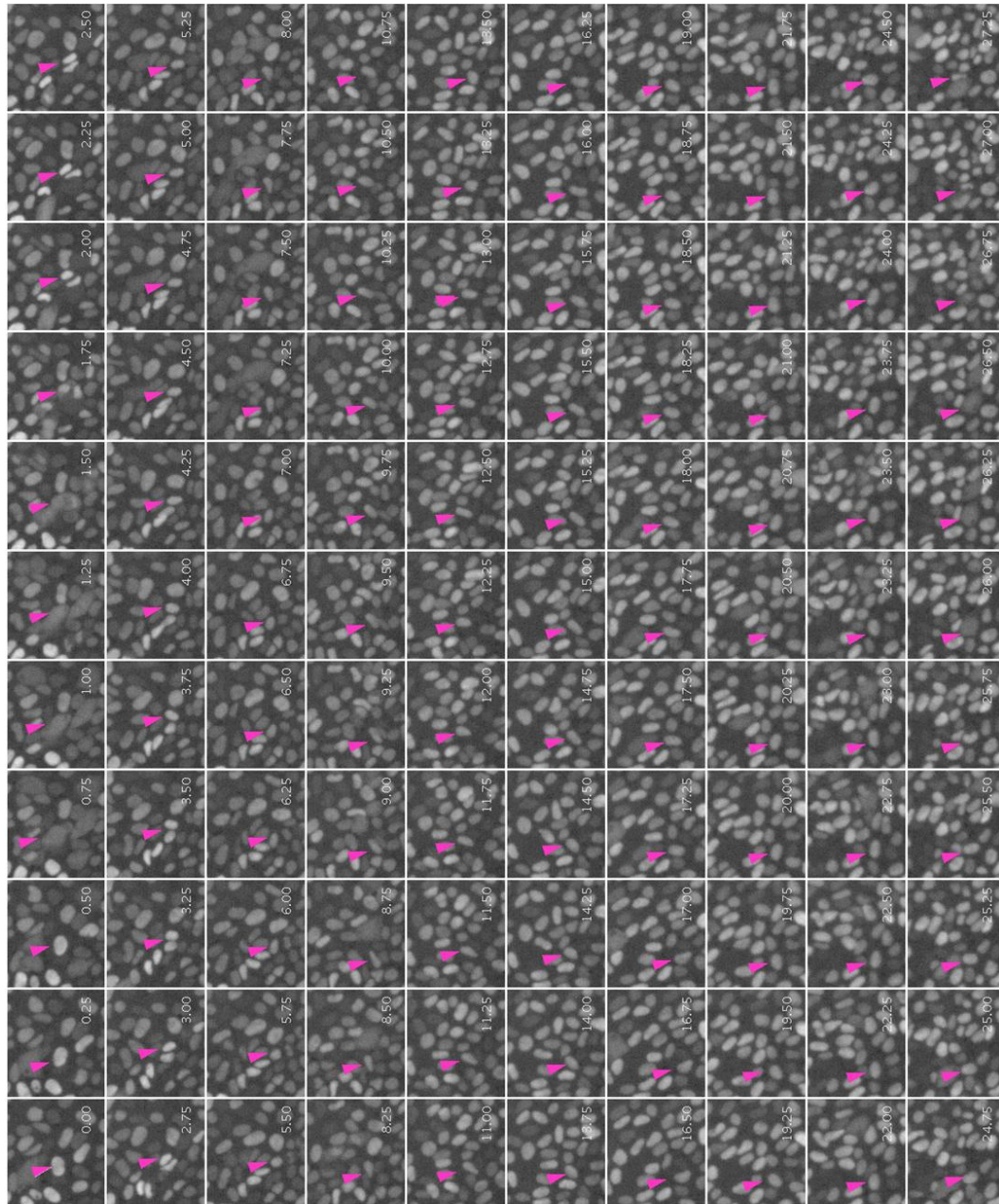
Figure 7: Fucci Orange and SKP2 expression are not mutually exclusive in undifferentiated hESC. Enumerated arrows: 1, bright Fucci Orange cells maintain SKP2 expression, even outside of the colony; 2, Fucci Orange positive cells show reduced levels of SKP2 expression

SKP2 to S through M phase, then there would be an apparent decrease of the number of SKP2-positive/Fucci Orange-negative cells since the population of S-M phase residing cells effectively decreases as G1 extends.

In an attempt to elucidate the expression pattern of SKP2 within hESC, we created a series of SKP2 fusion protein sensors to report SKP2 degradation patterns. We created three variants encoding different lengths of the N-terminal sequence of SKP2 fused downstream of mAG, a green fluorophore. mAG SKP2-11, mAG SKP2-50, and mAG SKP2-80 contain the first 11, 50, and 80 amino acids of human SKP2, respectively (Figure 8A). Amino acids 64-75 in SKP2 were thought to encode a putative NLS to localize SKP2 to the nucleus. Stable hESC lines carrying one of each of the SKP2 fusion reporters demonstrated that the NLS is located between residues 50 and 80; the mAG SKP2-11 and SKP2-50 fusions were both cytoplasmic, and the mAG SKP2-80 version showed tight nuclear localization, as shown in Figure 8B. Each sensor variant included the degradation sequence responsible for cell cycle specific degradation (the D-box). The nuclear localization of the SKP2-80 version permitted stable hESC carrying this fusion sensor to be tracked via live time-lapse imaging, and the intensity of sensor fluorescence within a single cell quantified for the duration of the imaging time course. The intensity of the mAG-SKP2-80 sensor appears to drop rapidly in mitotic cells, but is expressed at low levels throughout the remainder of the cell cycle (Figure 8C, 8D). These observations suggest that SKP2 may be ubiquitously expressed throughout the entire cell cycle of hESC with only modest fluctuations in expression levels.



**Figure 8: Expression pattern of SKP2 sensor.** **A**, SKP2 fusion sensor constructs. **B**, mAG-SKP2 stable sensor lines demonstrating cytoplasmic localization of mAG Skp2-11 and mAG Skp2-50, and nuclear localization of mAG Skp2-80 sensor. **C**, mAG-SKP2-80 sensor intensity in hESC in a single hESC reporter line derived from live time-lapse imaging. **D** (next page): Montage of single tracked mAG-SKP2-80 sensor in hESC colony over course of time-lapse live imaging used to create intensity plot of panel **C**.



D

### Differentiating hESC show increased Fucci Orange expression

We used time-lapse imaging of stable Fucci Orange reporter hESC to address questions regarding the kinetics of G1 lengthening, and the spatial occurrence of cells expressing Fucci Orange within and outside of colonies. Time-lapse imaging of Fucci Orange hESC demonstrates that compounds known to induce

differentiation of hESC<sup>85</sup> (DMSO, HMBA; Figure 9A, 10E; 10B) cause an increase in Fucci Orange expression in both reporter cell lines. LY294002 is a PI3K inhibitor<sup>106</sup>, and RRD is a small molecule inducer of G1 arrest<sup>73</sup>. Both compounds cause increased Fucci Orange expression (Figure 9C, 10D). These compounds show dose-responsiveness to Fucci Orange expression via live-cell imaging, with the proportion of Fucci Orange-positive cells increasing alongside the concentration of compound. Time-to-peak kinetics of Fucci Orange expression varies with the compound used; DMSO produces a later peak at approximately three days of treatment, with HMBA, RRD and LY294002 all producing peaks in approximately half that time, after 1.5 days of treatment. Regardless of the time required to reach peak Fucci Orange expression, the shape of the Fucci Orange response curve follows a typical bell-shaped distribution, with a plateauless peak quickly tapering to lower Fucci Orange-positive cell numbers by the end of the treatment course. Fucci Orange expression appears to be a very early indicator of differentiation, detectable as early as 12-16 hours after treatment of hESC with 1.0% DMSO, 3 mM HMBA, 40 uM RRD-251 and 40 uM LY294002 (Figure 9).

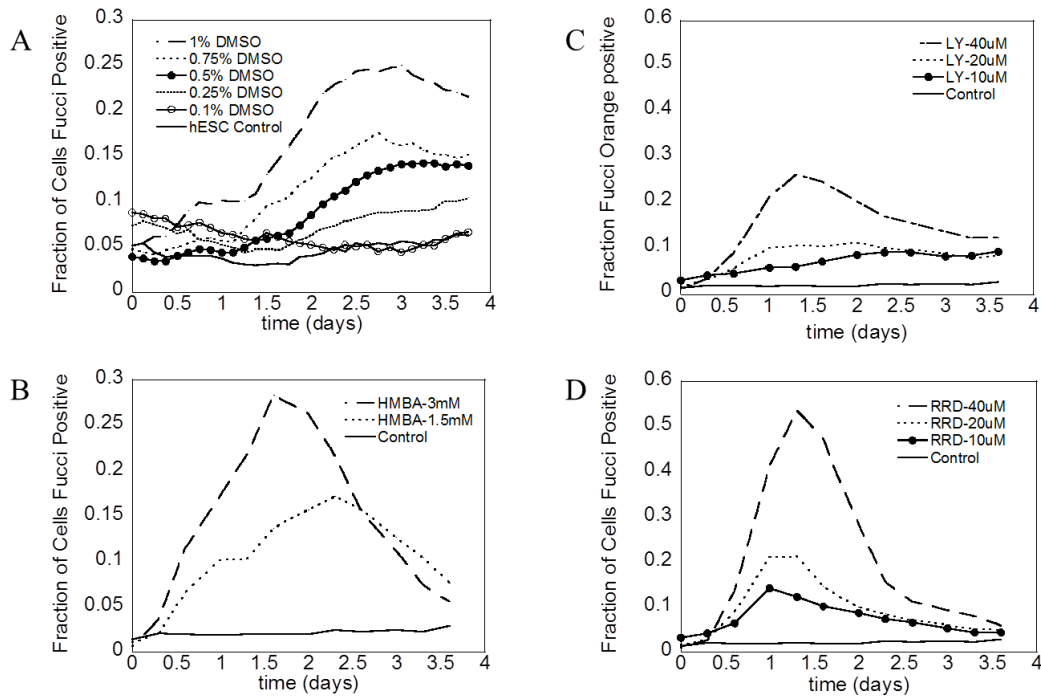
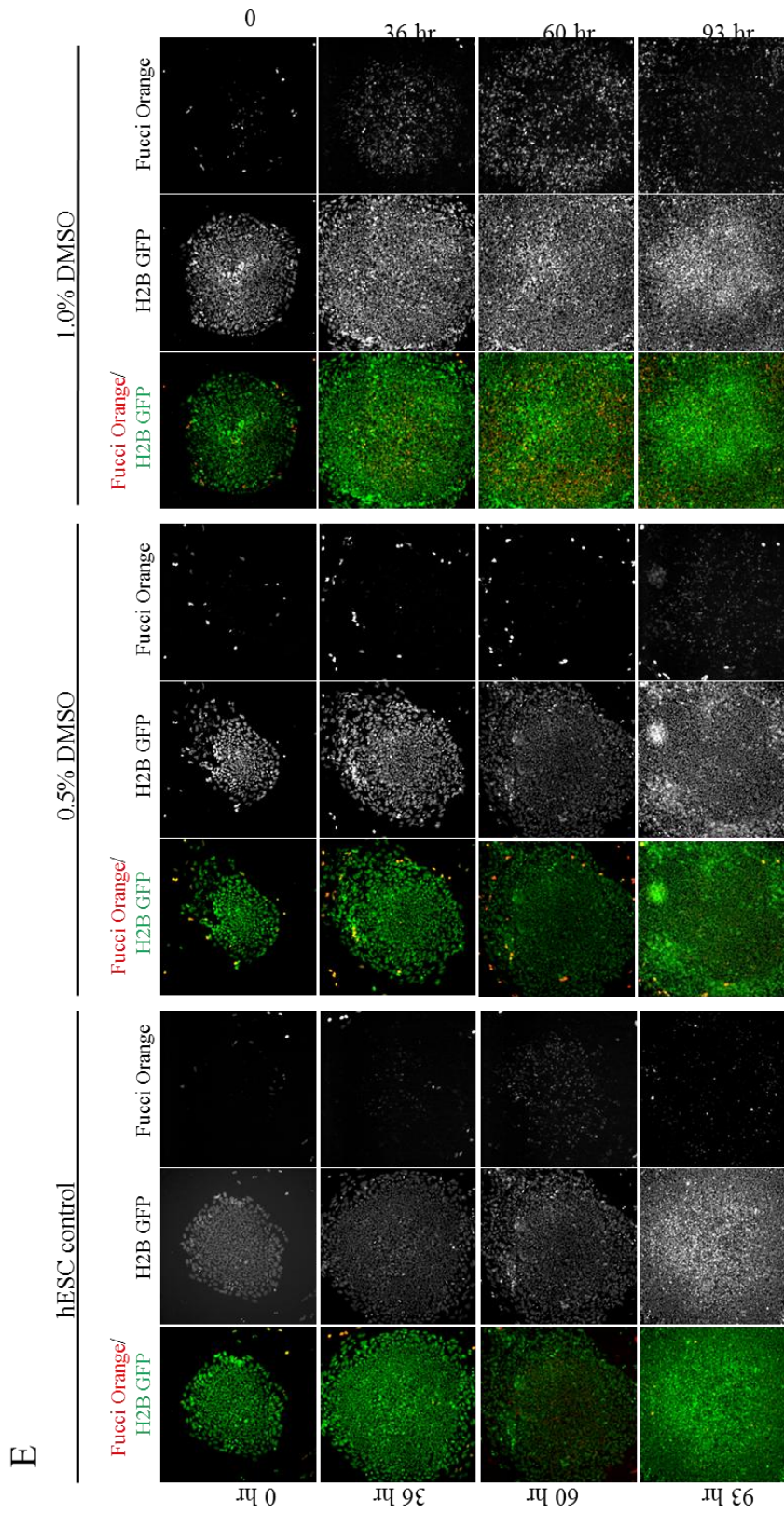


**Figure 9: Fucci Orange expression increases under differentiation conditions and is dose-dependent.** A, B: Live time-lapse imaging demonstrates that compounds initiating differentiation of hESC (DMSO, HMBA) and C, D: G1-arrest (LY294002, RRD) cause an increase of Fucci Orange expression. E: representative images from DMSO dose curve demonstrating Fucci Orange expression increases with time and concentration.



Lengthened G1 indicates loss of pluripotency

Fucci Orange expression is increased following differentiation with compounds 1.0% DMSO, 3 mM HMBA, 40  $\mu$ M RRD-251, 40  $\mu$ M LY294002 and  $10^{-5}$  M RA (Figure 9). When hESC are treated for 48 hours with these compounds and undifferentiated and vehicle controls, the Fucci Orange-positive fraction of cells are more likely to be negative for OCT4 expression (Figure 10). H9 Fucci Orange-positive cells are between 68 – 91% OCT4-negative, and 61 - 91% of Fucci Orange-positive cells are negative for OCT4 in the H1 line.

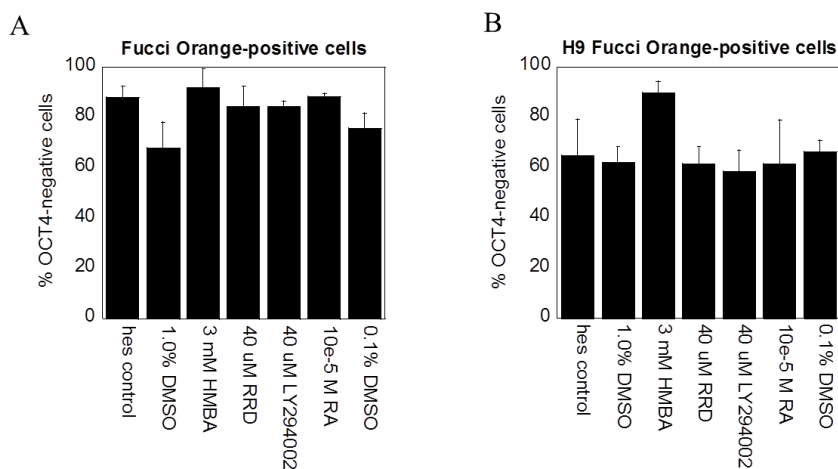


**Figure 10: Fucci Orange-positive cells are more likely to be OCT4-negative.** hESC residing in G1 are more likely to have lost pluripotency marker OCT4 expression. A, B: Both H1 and H9 Fucci Orange-positive cells are more likely to be negative for pluripotency marker OCT4 following 48 hours of differentiation with a panel of compounds and controls.

Bars represent data from multiple wells, approximately 320,000 cells on average.

Pluripotent hESC are characterized by expression of the cell surface markers Tra-1-60 and SSEA-3, both of which are tightly associated with the pluripotent state<sup>138</sup> and are downregulated upon the onset of differentiation<sup>85</sup>. Fucci Orange hESC were differentiated for 2 days with a variety of compounds and were then assayed by flow cytometry for Tra-1-60 or SSEA-3. Fucci Orange-positive cells are more likely to be negative for pluripotency markers Tra-1-60 and SSEA-3 than they are to be positive for these markers (Figure 11), suggesting that lengthened G1 indicates exit from the pluripotent state. A smaller proportion of Fucci Orange-positive cells are positive for these two cell surface markers, likely owing to the fact that pluripotent cells are cycling and therefore a small percentage of this population will reside G1.

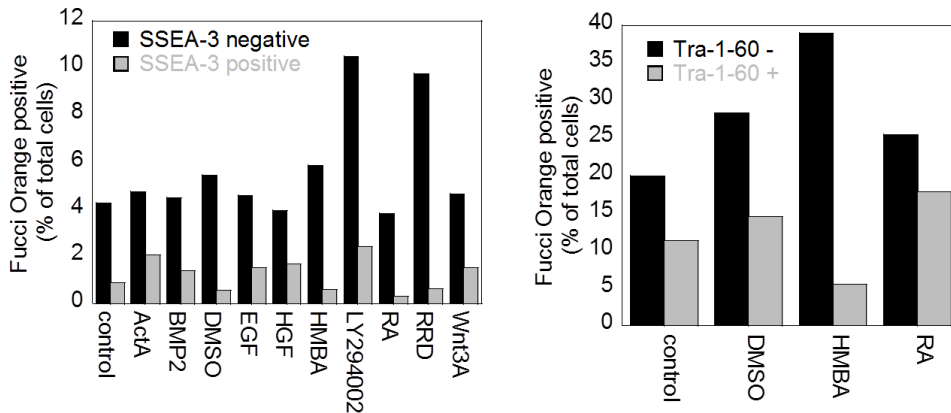


**Figure 11: Fucci Orange positive cells are more likely to be negative for pluripotency-related cell surface markers SSEA-3 and Tra-1-60.** Fucci Orange positive cells show loss of cell surface pluripotency markers SSEA-3 and Tra-1-60 following 48 hours treatment with differentiation agents.

We explored the G1 and the pluripotent compartment in further detail using Fucci Orange hESC differentiated 2 days with 1.0% DMSO and stained for OCT4 expression. Approximately 80% of OCT4-positive cells are Fucci Orange-negative (Figure 12) and the remaining 20% of cells are double positive for OCT4 and Fucci Orange expression.

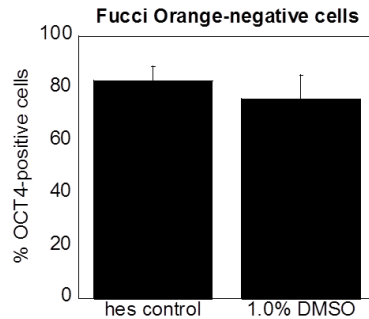


**Figure 12: OCT4 positive cells are more likely to be Fucci Orange negative.** Pluripotent cells are more likely to reside outside of G1 compared to hESC that have lost OCT4 expression. A small proportion (approximately 20%) of cells in both control and DMSO-induced hESC co-express Fucci Orange and OCT4 protein. Bars represent data from multiple wells, approximately 320,000 cells on average.

The OCT4 and Fucci Orange double positive most likely represent cycling pluripotent hESC in G1, a result in concordance with previous observations. Alternatively, these double positive cells may have acquired lengthened G1 in the early stages of differentiation but have not yet decreased OCT4 levels.

We next asked if the correlation between lengthened G1 and loss of pluripotency could be detected across entire colonies of differentiated hESC. Scanned plates of Fucci Orange hESC stained for OCT4 protein were subject to automated image analysis to identify and segregate colonies of hESC. Custom, automated scripts identified colonies based on cellular proximity; cells within colonies grow tightly together while differentiated cells outside of the colony are further spaced apart. hESC colonies are comprised of closely-associated cells with large nucleus-to-cytoplasm ratios. Differentiated cells lying outside of pluripotent colonies tend to be scattered, and have increased cellular size and smaller nucleus-to-cytoplasm ratios compared to their pluripotent counterparts. These features of pluripotent versus differentiated hESC means that nuclei growing in close proximity to one another are generally found within pluripotent colonies, while greater distances between adjacent nuclei indicate differentiated hESC growing outside of a colony. After colonies are identified based on tight nuclear proximity, the mean intensity of Fucci Orange reporter or OCT4 immunofluorescence intensity calculated for the whole colony. Image analysis of cultures grown for 48 hours in the presence of 1.0% DMSO, 3 mM HMBA or undifferentiated control show the same correlation observed for single cells between increased Fucci Orange expression and loss of pluripotency also exists for entire colonies. The inverse relationship between OCT4 fluorescence and Fucci Orange levels is represented in Figure 13.

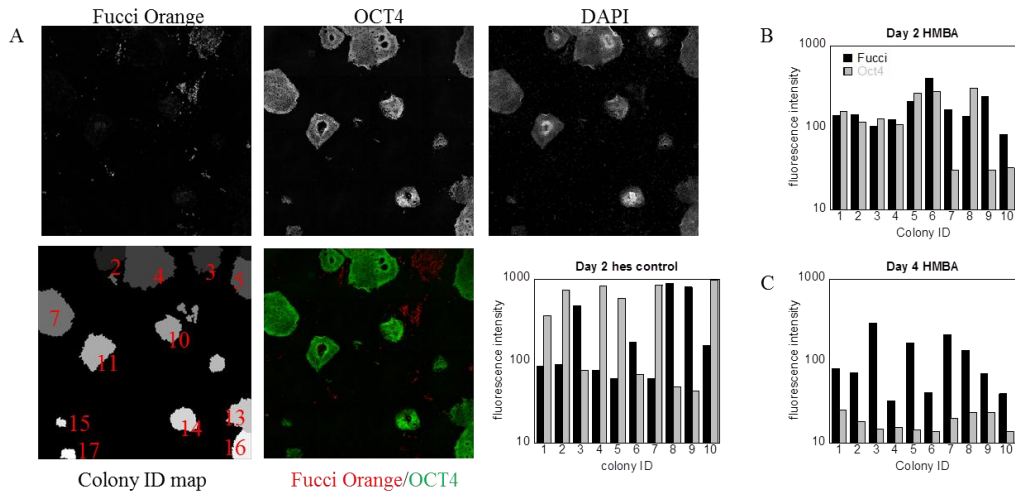


**Figure 13: Automated colony analysis reveals an inverse relationship between Fucci Orange expression and OCT4 across entire colonies.** A: Colonies are identified via automated image analysis via cell-cell proximity. Mean fluorescence intensity of Fucci Orange and OCT4 expression is calculated for each colony. Lengthened G1 and pluripotency are inversely related across colonies. B,C: 2 days differentiation with HMBA causes upregulation of Fucci Orange while OCT4 levels are maintained. After 4 days treatment with HMBA, OCT4 levels are reduced, suggesting this method of differentiation is mediated by an increase in G1 length followed by loss of pluripotency.

To determine if changes in pluripotency occurred at the mRNA level, Fucci Orange cells were either differentiated with 1.0% DMSO or permitted to extensively spontaneously differentiate, and were separated into Fucci Orange-positive and negative populations by FACS. Fucci Orange-positive cells treated with DMSO show slightly decreased expression levels of pluripotency genes *SOX2* and *REX1*, and highly upregulated levels of genes associated with mesoderm differentiation, such as *EOMES*, *FOXA2*, *SOX17*, and *GATA4* (Figure 14A). Spontaneously differentiated Fucci Orange-positive cells show reduced levels of pluripotency markers *NANOG*, *SOX2*, and *REX1* relative to the Fucci Orange-negative population (Figure 14B).

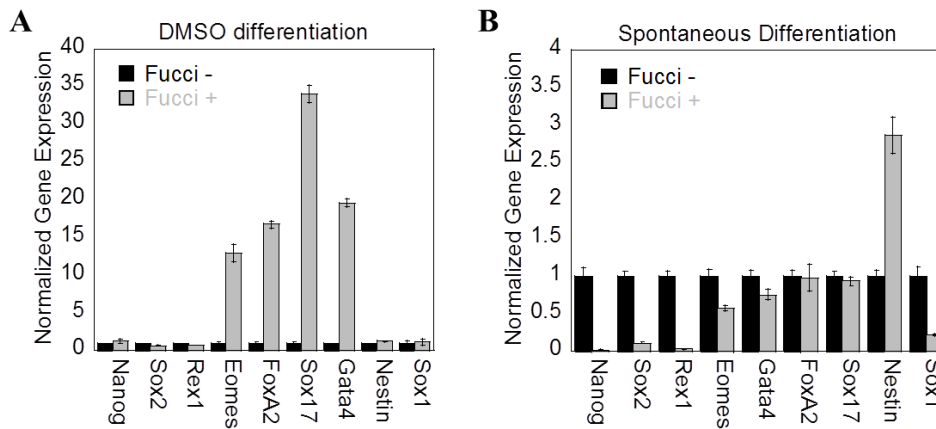


**Figure 14: Fucci Orange expression is correlated with a change in gene expression of pluripotent and differentiation markers.** Gene expression by qPCR on Fucci Orange-positive and -negative populations separated by FACS. **A:** DMSO treated Fucci Orange-positive cells show increased gain of differentiation markers. **B:** Fucci Orange cells arising spontaneously in culture show nearly equivalent gain of differentiation marker but greatly reduced levels of pluripotency related gene expression.

The ability to create a pluripotent colony is a functional characteristic of undifferentiated hESC, dependent on the ability to self-renew from an initial pluripotent state. Colony-initiating cells (CIC) assay provides an estimate of the pluripotent status within subsets of a population, and is assessed by staining for alkaline phosphatase activity, a sensitive marker of undifferentiated hESC<sup>139</sup>. We hypothesized that Fucci Orange-negative cells would contain more CICs compared to the Fucci Orange-positive fraction, in the light of our previous results that demonstrated Fucci Orange-positive cells are more likely to have lost pluripotency markers. Undifferentiated cultures of cells were isolated by FACS dependent upon the presence or absence of Fucci Orange expression. Fucci Orange-negative cells contain significantly more colony-initiating cells compared to populations of Fucci Orange-positive cells (Figure 15), when plated at the same density and under the same growth conditions, following FACS. The difference in

CIC frequency between the two sorted Fucci Orange populations suggests that Fucci Orange-negative cells are more likely to be pluripotent and capable of self-renewal, and therefore be able to give rise to a pluripotent colony when directly compared to Fucci Orange-positive cells. The ability of Fucci Orange-positive cells to form pluripotent colonies suggests that there is a population of hESC residing in G1 that have maintained pluripotency or have not yet fully committed to a differentiation programme and are able to revert to a pluripotent state under favourable conditions.

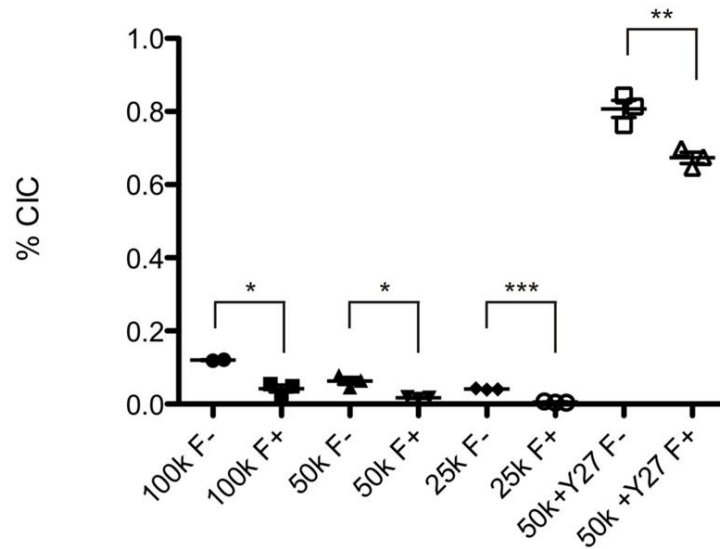


**Figure 15: Fucci Orange negative hESC populations contain more colony-initiating cells.** FACS isolated populations of Fucci Orange cells differentiated for two days with 1.0% DMSO show different rates of CIC between the two populations. Fucci Orange positive cells are less likely to be pluripotent, and show decreased rates of colony forming cells compared to Fucci Orange negative cells sorted from the same population.

### Lengthened G1 indicates gain of lineage markers

Given that Fucci Orange-positive cells show a loss of pluripotency markers after induction with small molecules and chemical compounds, we next asked if Fucci Orange expression would be increased following directed differentiation towards each of the germ layers, and if so, if Fucci Orange expression would correlate with lineage related markers. We used two experimental approaches to answer this question. First, we assayed gene expression by Q-RT-PCR on sorted populations of differentiated Fucci Orange cells. FACS isolated populations show increased gene expression of lineage-related markers after differentiation towards each of the three lineages (mesoderm, endoderm, and ectoderm) in the Fucci Orange-positive population compared to the Fucci Orange-negative population

(Figure 16). These same populations show a reduction in pluripotency markers OCT4, NANOG, and SOX2 in the Fucci Orange-positive population in most directed lineage differentiations. SOX2 and OCT4 expression is maintained in the Fucci Orange-positive population of neural precursor cells, in contrast to the endoderm and mesoderm differentiated Fucci Orange-positive fraction. This result is not surprising, given that these pluripotency genes have been demonstrated to be maintained in, and required for differentiation to early neural precursor populations<sup>140,141</sup>.

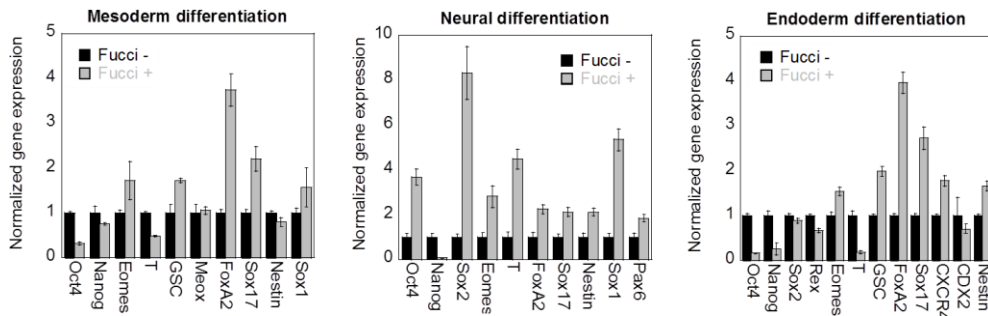


**Figure 16: Fucci Orange expression correlates with a gain of lineage-related gene expression.** FACS isolated populations show an increase of lineage markers (mesoderm, endoderm, ectoderm) in the Fucci Orange-positive fraction compared to the Fucci Orange-negative population. These same populations show a reduction in most pluripotency markers in the Fucci Orange-positive population.

Second, we used HCS to assay Fucci Orange hESC differentiated towards an endoderm fate. Cells showed a strong correlation between endoderm markers GATA4 and TCF2 in the Fucci Orange-positive fraction when examined by indirect double immunofluorescence. Cells positive for endoderm markers GATA4 and TCF2 are more likely to be Fucci Orange-positive (Figure 17B, 16C). OCT4-positive cells are more likely to be Fucci Orange-negative (Figure 17A), while EOMES-positive cells are approximately equally likely to be either positive or negative for Fucci Orange expression (Figure 17D). Together, this data suggests that Fucci Orange expression can indicate gain of endoderm lineage and loss of pluripotency. The lower correlation of Fucci Orange expression within the EOMES-positive fraction is consistent with this gene representing a marker of early endoderm progenitor cells that have not yet acquired a lengthened G1 phase.

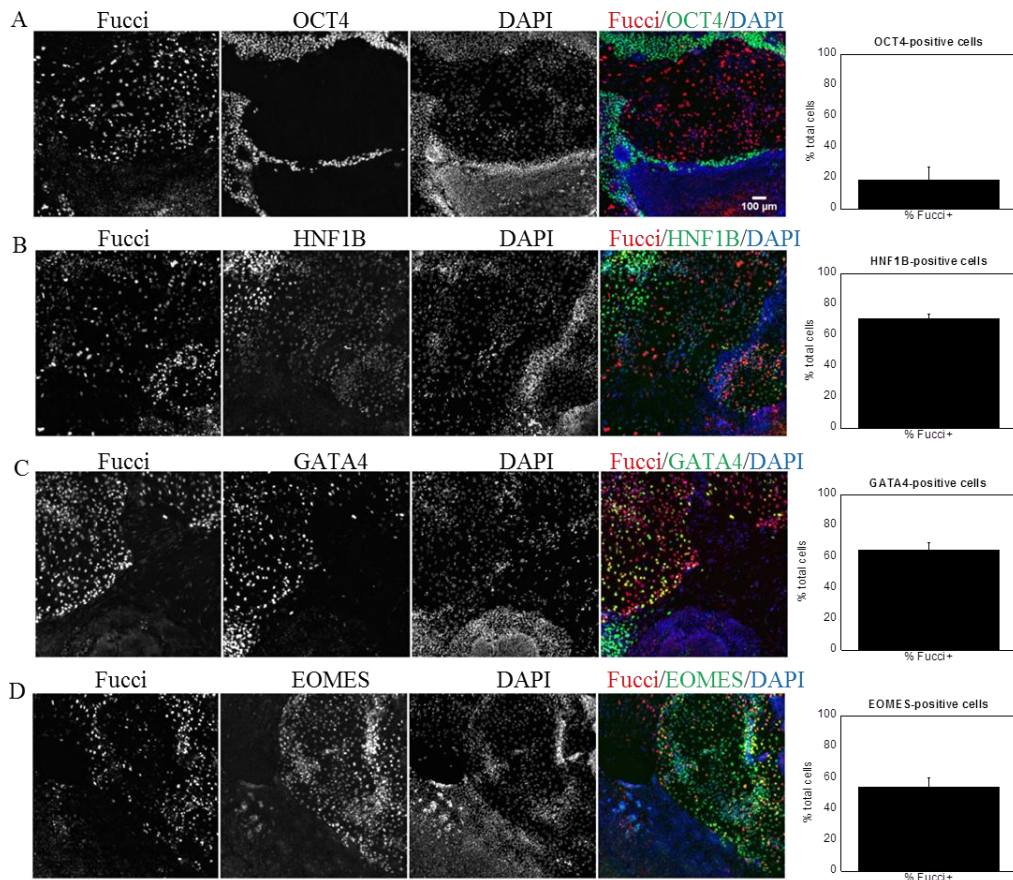


**Figure 17: Endoderm markers are more likely to be Fucci Orange positive.** Indirect immunofluorescence shows a correlation between endoderm markers (GATA4, TCF2) and Fucci positive cells after differentiation towards the endoderm lineage. EOMES is less strictly correlated with increased Fucci Orange expression, suggesting this transcription factor may mark an early progenitor population that has maintained a shortened G1.

## Discussion

Work to date establishing relationships between changes in cell cycle parameters of differentiating hESC have demonstrated a correlation between length of G1 and loss of pluripotency within bulk cultures. This work has been carried out using traditional cell cycle analysis profiling, and limited use of immunofluorescence against cell cycle markers to establish broad trends in entire populations of cells. Differentiation protocols used to date have relied on limited use of DMSO, the CDK2 inhibitor Roscovitine, embryoid body formation, and spontaneous differentiation.

Here, for the first time, we have: 1) established two novel cell cycle reporters in hESC and utilized them in live-cell tracking and HCS imaging contexts to quantify numbers of G1-residing cells, length of G1, and the kinetics of cell cycle changes in pluripotent and differentiating cells; 2) demonstrated lengthened G1 indicates loss of pluripotency by use of compounds that induce differentiation, including a PI3K inhibitor, DMSO, HMBA and RA; and, 3) correlated lengthened G1 as an indicator of differentiation across all three germ layers on the level of gene expression, and protein expression for endoderm precursors.

### Use of Fucci Orange in hESC

Fucci Orange can be stably transfected into hESC lines and used as a reliable indicator of G1-status of individual cells. Indirect immunofluorescence of Cyclin B1 protein and Hoechst nuclear staining demonstrate that Fucci Orange expression is limited to G1 phase (Figure 5). Single cell tracking of CAG-H2GFOIP transgenic lines shows that Fucci Orange expression is increased immediately following mitosis and quantifies total cell cycle time of 17 hours with a 2.5 hour G1 length in an undifferentiated cell, in agreement with published data to date (Figure 4C). Indirect immunofluorescence data presented here regarding ubiquitous expression of SKP2 within hESC is in agreement with published accounts<sup>37</sup> (Figure 7). Co-expression of SKP2 and its target Cdt1 was not expected based on current knowledge of cell cycle regulation of these two proteins. It is possible that SKP2 may be subject to unique regulation within the pluripotent hESC population that permits its expression during G1 but prevents any E3 ligase activity, thus allowing SKP2 to be co-expressed with Fucci Orange. Unique regulation of cell cycle regulatory proteins involved in protein degradation is not unprecedented in embryonic stem cells; mESC exhibit Geminin protein expression throughout the complete cell cycle, including G1, when it is

normally degraded in somatic cells<sup>142</sup>. How Geminin is maintained in G1 of pluripotent mESC has not been determined, but it does demonstrate that unique pathways mediating pluripotency and interrupting typical phasic expression of cell cycle molecules can exist within pluripotent cell populations. Future work examining the activity of this proteasome mediator may reveal interesting pathways controlling pluripotency and cell cycle modification in hESC.

Time-lapse imaging of Fucci Orange cells demonstrates that conditions leading to differentiation or G1-arrest cause a dose-dependent increase in Fucci Orange expression relative to undifferentiated conditions. Kinetics of Fucci Orange expression upon 1.0% DMSO treatment show the first noticeable increase occurring at approximately 1.5 days of growth in DMSO-containing medium, a value in close agreement to kinetics of DMSO-induction of MEL cells<sup>76</sup>. Early work with DMSO-differentiated MEL cells demonstrated that these cells were committed to differentiation after 30 hours exposure to DMSO, suggesting a series of events must occur before a fate decision is made. Studies using HMBA to induce MEL differentiation showed differentiation-related gene expression could be detected in the second G1 following addition of HMBA<sup>87</sup>. Similarly, hESC cultured with 3 mM HMBA show a peak in Fucci Orange expression at 1.5 days, or approximately 2 full pluripotent cell cycles, following HMBA induction (Figure 9B). Currently, the only published kinetic data relating to cell cycle changes and differentiation of hESC shows that 72 hours of differentiation by growth under feeder-free conditions with incomplete growth media is required to see a reduction in OCT4 protein and a decrease in the number of cells residing in S-phase.

#### Lengthened G1 indicates loss of pluripotency

Fucci Orange hESC undergoing differentiation show increased expression of the Fucci Orange reporter. Examination of individual cells positive for Fucci Orange expression shows these cells are more likely to be negative for pluripotency markers OCT4 (Figure 10, Figure 12), and SSEA-3 and Tra-1-60 (Figure 11) after 48 hours of treatment. Initial work in cell cycle changes of differentiating hESC demonstrated large scale changes of OCT4 protein expression correlated to increase in cell cycle length by BrdU or propidium iodide incorporation. Western blot analysis of OCT4 protein levels showed noticeable decrease in Day 5 EBs; Day 10 EBs showed similar levels of OCT4 protein with approximately 47% of cells residing in G1.<sup>37</sup> hESC differentiated for 24 or 48 hours with incomplete media show 80-90% of cells are positive for OCT4 by antibody staining, with approximately 50% of cells residing in S-phase. Noticeable cell cycle and OCT4

level changes do not occur until 72 hours of differentiation in this system, when 12% of cells within the culture are OCT4-positive and 10% of the population resides in S-phase<sup>143</sup>. Spontaneously differentiated hESC in 6 day old cultures show cells positive for the cell surface pluripotency marker GCTM-2 are 90% OCT4-positive and 20% of this population resides in G1; cells negative for GCTM-2 are less than 10% OCT4-positive and 60% of this population is in G1<sup>48</sup>. The work presented here clearly establishes much earlier changes in pluripotency markers and cell cycle profile in early differentiating hESC. The Fucci Orange reporter system is a sensitive indicator of the early steps of loss of pluripotency of hESC, with increase in Fucci Orange expression first clearly detectable above control levels at 0.5-1.0 days of differentiation. By 48 hours of differentiation with DMSO, HMBA, RRD-251 and LY294002 show peak expression of Fucci Orange (Figure 9), and the Fucci Orange-positive population expresses greatly decreased levels of pluripotency markers OCT4, SSEA-3 and Tra-1-60 (Figure 12, 12). Together these data suggest that changes in G1 length of hESC can indicate very early loss of pluripotency in hESC and is more sensitive to early detection of differentiation than reading out cell cycle profile by BrdU incorporation.

Spontaneous or DMSO-induced differentiation induces a loss of pluripotency gene expression or gain of differentiation-related gene expression in the Fucci Orange-positive population isolated by FACS (Figure 14). The difference in gene expression profiles between the two types of induction suggest that hESC may choose to extend G1 via two different mechanisms, with correlation in increased gene expression related to acquisition of a differentiated fate, or with downregulated pluripotency-related genes. Alternatively, the difference in expression of pluripotency versus differentiation-related genes between the two experiments may represent different stages of differentiation, with upregulation of DMSO-induced mesoderm genes occurring before decreased expression of pluripotency related genes as a early stage of differentiation, while the spontaneously-differentiated gene expression profile may represent a later stage of differentiation where loss of pluripotency is decreased relative to increased expression of differentiation-related genes. The high expression of *NESTIN* alongside low *SOX2* and *OCT4* expression within the Fucci Orange-positive spontaneously differentiated population may be reflective of the pleiotropic role of *NESTIN* in both neural and pancreatic cell differentiation<sup>144-146</sup>.

Lengthened G1 can indicate loss of pluripotency by spontaneous or compound-induced differentiation of hESC. Fucci Orange expression can be used to detect very early changes in protein and gene expression indicators of

pluripotency and has shown greater sensitivity to these changes than previously appreciated in current accounts of cell cycle changes in hESC.

#### Lengthened G1 indicates gain of lineage

Fucci Orange-positive cells show increased lineage gene expression following directed differentiation and isolation by FACS. Endoderm differentiation by an established protocol<sup>128</sup> shows increased expression of expected endoderm-related genes *SOX17*, *FOXA2*, and *CXCR4* in the Fucci Orange-positive fraction as demonstrated in the original paper. *BRACHYURY* and *GSC* are upregulated to a lesser extent, likely because these genes are associated with epithelial-to-mesenchyme transition, and are turned on early in the initial differentiation process and downregulated by the early endoderm stage. *EOMES* is increased for both gene expression and protein level in the Fucci Orange-positive fraction (Figure 16, 18).

Neural differentiation<sup>129</sup> has shown expected results of increased expression of *SOX1*, *PAX6*, and *NESTIN* and decreased *NANOG* expression out of the genes studied in the original paper. Our results show increased expression of *OCT4* and *SOX2* genes, both of which are associated with neural differentiation and thus do not seem unexpected. However, several non-neural genes are expressed at higher levels in the Fucci Orange-positive population relative to the Fucci Orange-negative population, including EMT-related genes *FOXA2*, *EOMES*, *T*, and *SOX17*. The difference in the gene expression profiles of the neural precursor populations derived in the published paper and in our experiment may be due to the difference in length of treatment (10 days versus 5 days, respectively), cell line used (H9 wild type cells versus H1 Fucci Orange reporter line, respectively), or compounded by method of analysis, presenting entire treated population relative to the untreated control in the original protocol compared to our analysis that presented Fucci Orange-positive cell transcript levels relative to the Fucci Orange-negative population.

Early mesoderm differentiation is characterized by increased expression of *EOMES* and decreased *OCT4* and *NANOG*<sup>147</sup>. Our data shows these expected mesoderm changes in the Fucci Orange-positive population relative to the Fucci Orange-negative population, but also increased expression of early endoderm markers *SOX17* and *FOXA2*. Increased expression of these typical endoderm markers suggests that our cells have differentiated towards a mesendoderm precursor<sup>148</sup>. The protocol used for this experiment was derived for differentiation of human embryoid bodies to give rise to haematopoietic precursors<sup>130</sup>, and we instead cultured our cells as an adherent monolayer on MEFs. It is possible that

our results do not generate a pure mesoderm population due to the difference in application of the protocol.

Here we have clearly shown for the first time that lengthened G1 is an indicator of gain of lineage function across each of the three germ layers. Fucci Orange-positive cells are enriched for markers of endoderm protein and gene expression, and for lineage related genes for neural and mesoderm lineages. Given that we have demonstrated that Fucci Orange is an early and sensitive indicator of loss of pluripotency following compound based differentiation, it would be useful to test early arising populations of lineage precursor cells to see if lengthened G1 can be used to study the first steps of lineage commitment. Kinetics of Fucci Orange expression and correlation of lineage markers may reveal important first steps in generating established germ layer populations that have been previously unappreciated due to the necessary length of time required before bulk populations of differentiating hESC show detectable lineage characteristics.

#### Caveats and considerations

Cdt1 is recruited to sites of DNA damage to initiate repair, even outside of G1 when it is typically expressed. Initiation of Cdt1-based repair at damage sites requires an intact N-terminus PIP-box sequence (residues 3-10) to associate with chromatin-bound PCNA. Without this sequence, Cdt1 cannot be recruited to the damage site and degraded following repair initiation. To date, the mechanism of how Cdt1 is released from cell cycle-dependent degradation to permit DNA repair activity is unknown. Fucci Orange does not contain the required PIP-box motif to associate with PCNA, and therefore it cannot be recruited to DNA damage sites. Full length Cdt1 is post-translationally regulated by three independent pathways, and of these, only the SCF<sup>Skp2</sup> pathway functions to degrade the Fucci Orange reporter. If DNA damage triggers release of Skp2-dependent proteasome degradation, then irradiation or use of compounds causing DNA breaks, rather than differentiation coupled with lengthened G1, could be responsible for increased Fucci Orange expression.

Non-specific effects of small molecules can be confounding variables when interpreting data. It is likely that compounds DMSO, HMBA, RRD-251 and LY294002 could affect multiple pathways within hESC. If these compounds were inhibiting proteasome function, for example, and decreasing protein degradation, it is likely cell cycle arrest would occur. If such off-target effects were occurring with treatment of hESC with any of these compounds, cells would arrest in the cell cycle phase they were residing in at time of treatment. Without the ability to degrade proteins and transit to the next cell cycle phase, an increase in Fucci

Orange expression would be detected, due to the constitutive expression of the reporter driven by the CAG promoter. Studies of inhibition of proteasome by chemical compounds<sup>149,150</sup>, mutation<sup>151</sup>, or inhibition of cell cycle protein degradation<sup>152</sup>, show that cells lacking protein degradation exhibit cell cycle arrest, and once released from this metabolic block, show DNA re-replication, apoptosis, and aberrant cellular division with daughter cells of varying size and DNA content. Given that chemically treated hESC show an increase in percentage of cells positive for Fucci Orange expression, it does not seem likely that observed effects of the chemicals used in these studies can be attributed to proteasome inhibition. Examination of DNA re-replication and proper DNA content of daughter cells following chemical induction could further eliminate altered protein degradation as an explanation for the observations reported here.

Our results permit the use of lengthened G1 as a lineage unbiased indicator of loss of pluripotency and onset of differentiation in hESC. As an early indicator of loss of pluripotency, lengthened G1 status can be used to isolate populations of early precursor cells to study early fate decisions. Identification of early precursor populations will facilitate optimization of directed differentiation protocols to generate pure lineages for use in clinical settings. Lineage unbiased indication of differentiation will permit HCS of compounds not limited to a subset of cell types, thus reducing the number of input cells needed while maximizing the potential for hits. Given that Fucci Orange expression increases in hESC treated with compounds intended for chemotherapeutic use (HMBA<sup>96</sup> and RRD-251<sup>74</sup>), lengthened G1 in hESC may be a useful tool for identifying novel anti-cancer drugs.

#### Future work

Given the unusual cell cycle properties of hESC and established ties between changes in cell cycle phase lengths and differentiation within multiple cell types, developmental stages, and species, it is not surprising that hESC utilize unique mechanisms of cell cycle regulation that also maintain pluripotency. Future work clearly demonstrating the expression profiles of pluripotent cells compared to those cells initiating or having undergone differentiation is necessary to understand the contradictions presented in the current literature. Studying the kinetics of cell cycle change and length of G1 acquisition between the three germ layers may reveal intriguing developmentally-relevant cues to assist in enriching populations of cells for directed differentiation programmes. Here we have established the use of a live fluorescent cell cycle reporter capable of identifying early differentiation towards all three germ layers that may have broad application

towards studying the kinetics and mechanisms of early fate decisions, as well as serving as a tool in HCS for discovery of small molecules that induce lineage differentiation or chemotherapeutic agents. The Fucci Orange reporter provides two advantages over HCS methods in hESC used to date. First, a reporter indicating a biological change by gain-of-signal, rather than loss of signal (ie, by OCT4-GFP reporters or by immunofluorescence against endogenous OCT4 protein levels) are preferred for technical reasons. A gain of fluorescence signal is more detectable and sensitive than reading a loss of signal. Given we have demonstrated that Fucci Orange levels increase in all types of hESC differentiation (from general loss of pluripotency or gain of any of the three lineages), this reporter is able to indicate early changes in hESC identity in a non-specific manner that is highly sensitive. Secondly, most live fluorescent reporters used in hESC to date for HCS suffer from promoter silencing, creating difficulties in both maintaining a pure population of accurately reporting cells, and also potentially leading to false positives or missed hits due to misinterpretation of an apparent OCT4 signal. The Fucci Orange reporter has been maintained in hESC for up to 9 months with no noticeable loss of signal, and the CAG promoter is not subject to silencing within this cell type. Therefore, the CAG-Fucci Orange system represents a comprehensive, sensitive, and reliable means of detecting loss of pluripotency within hESC.

## References

- 1 Becker, K. A. *et al.* Self-renewal of human embryonic stem cells is supported by a shortened G1 cell cycle phase. *Journal of Cellular Physiology* **209**, 883-893 (2006).
- 2 Knoblich, J. A. *et al.* Cyclin E controls S phase progression and its down-regulation during Drosophila embryogenesis is required for the arrest of cell proliferation. *Cell* **77**, 107-120 (1994).
- 3 Edgar, B. A., Kiehle, C. P. & Schubiger, G. Cell-cycle control by the nucleocytoplasmic ratio in early drosophila development. *Cell* **44**, 365-372 (1986).
- 4 Murakami, M. S., Moody, S. A., Daar, I. O. & Morrison, D. K. Morphogenesis during Xenopus gastrulation requires Wee1-mediated inhibition of cell proliferation. *Development* **131**, 571-580 (2004).
- 5 Newport, J. & Kirschner, M. A major developmental transition in early xenopus embryos: characterization and timing of cellular changes at the midblastula stage. *Cell* **30**, 675-686 (1982).
- 6 Yarden, A. & Geiger, B. Zebrafish cyclin E regulation during early embryogenesis. *Dev. Dyn.* **206**, 1-11 (1996).
- 7 Lawson, K. A., Meneses, J. J. & Pedersen, R. A. Clonal analysis of epiblast fate during germ layer formation in the mouse embryo. *Development* **113**, 891-& (1991).
- 8 Macauley, A., Werb, Z. & Mirkes, P. E. Characterization of the unusually rapid cell cycles during rat gastrulation. *Development* **117**, 873-883 (1993).
- 9 Kiessling, A. A. *et al.* Genome-wide microarray evidence that 8-cell human blastomeres over-express cell cycle drivers and under-express checkpoints. *J. Assist. Reprod. Genet.* **27**, 265-276 (2010).
- 10 Braude, P., Bolton, V. & Moore, S. Human-gene expression 1st occurs between the 4-cell and 8-cell stages of preimplantation development. *Nature* **332**, 459-461 (1988).
- 11 Duman-Scheel, M., Weng, L., Xin, S. J. & Du, W. Hedgehog regulates cell growth and proliferation by inducing cyclin D and cyclin E. *Nature* **417**, 299-304 (2002).
- 12 Wong, C. C. *et al.* Non-invasive imaging of human embryos before embryonic genome activation predicts development to the blastocyst stage. *Nat Biotech* **28**, 1115-1121 (2010).
- 13 Stead, E. *et al.* Pluripotent cell division cycles are driven by ectopic Cdk2, cyclin A/E and E2F activities. *Oncogene* **21**, 8320-8333 (2002).
- 14 Buehr, M. *et al.* Capture of Authentic Embryonic Stem Cells from Rat Blastocysts. *Cell* **135**, 1287-1298 (2008).
- 15 Rosenstraus, M. J., Sundell, C. L. & Liskay, R. M. Cell cycle characteristics of undifferentiated and differentiating embryonal carcinoma cells. *Dev. Biol.* **89**, 516-520 (1982).
- 16 Ghule, P. N. *et al.* Reprogramming the pluripotent cell cycle: restoration of an abbreviated G1 phase in human induced pluripotent stem (iPS) cells. *Journal of Cellular Physiology*, n/a-n/a (2010).

- 17 Ruiz, S. *et al.* A High Proliferation Rate Is Required for Cell Reprogramming and Maintenance of Human Embryonic Stem Cell Identity. *Curr. Biol.* **In Press**, **Corrected Proof**, doi:DOI: 10.1016/j.cub.2010.11.049.
- 18 Zhang, L., Kendrick, C., Julich, D. & Holley, S. A. Cell cycle progression is required for zebrafish somite morphogenesis but not segmentation clock function. *Development* **135**, 2065-2070 (2008).
- 19 Kauffman, S. L. Lengthening of the generation cycle during embryonic differentiation of the mouse neural tube. *Exp. Cell Res.* **49**, 420-424 (1968).
- 20 Calegari, F. & Huttner, W. B. An inhibition of cyclin-dependent kinases that lengthens, but does not arrest, neuroepithelial cell cycle induces premature neurogenesis. *J. Cell Sci.* **116**, 4947-4955 (2003).
- 21 Calegari, F., Haubensak, W., Haffner, C. & Huttner, W. B. Selective lengthening of the cell cycle in the neurogenic subpopulation of neural progenitor cells during mouse brain development. *J. Neurosci.* **25**, 6533-6538 (2005).
- 22 Hiebert, S. W., Chellappan, S. P., Horowitz, J. M. & Nevins, J. R. The interaction of Rb with E2F coincides with an inhibition of the transcriptional activity of E2F. *Genes Dev.* **6**, 177-185 (1992).
- 23 Bartek, J., Bartkova, J. & Lukas, J. The retinoblastoma protein pathway and the restriction point. *Curr. Opin. Cell Biol.* **8**, 805-814 (1996).
- 24 Akiyama, T., Ohuchi, T., Sumida, S., Matsumoto, K. & Toyoshima, K. Phosphorylation of the retinoblastoma protein by CDK2. *Proc. Natl. Acad. Sci. U. S. A.* **89**, 7900-7904 (1992).
- 25 Carrano, A. C., Eytan, E., Hershko, A. & Pagano, M. SKP2 is required for ubiquitin-mediated degradation of the CDK inhibitor p27. *Nat. Cell Biol.* **1**, 193-199 (1999).
- 26 Tsvetkov, L. M., Yeh, K. H., Lee, S. J., Sun, H. & Zhang, H. P27(Kip1) ubiquitination and degradation is regulated by the SCFSkp2 complex through phosphorylated Thr187 in p27. *Curr. Biol.* **9**, 661-664 (1999).
- 27 Blomen, V. A. & Boonstra, J. Cell fate determination during G1 phase progression. *Cell. Mol. Life Sci.* **64**, 3084-3104, doi:10.1007/s00018-007-7271-z (2007).
- 28 Pfeuty, B., David-Pfeuty, T. & Kaneko, K. Underlying principles of cell fate determination during G(1) phase of the mammalian cell cycle. *Cell Cycle* **7**, 3246-3257 (2008).
- 29 Ruiz, S. *et al.* A High Proliferation Rate Is Required for Cell Reprogramming and Maintenance of Human Embryonic Stem Cell Identity. *Curr. Biol.* **21**, 45-52, doi:10.1016/j.cub.2010.11.049 (2011).
- 30 Clegg, C. H., Linkhart, T. A., Olwin, B. B. & Hauschka, S. D. Growth factor control of skeletal muscle differentiation: commitment to terminal differentiation occurs in G1 phase and is repressed by fibroblast growth factor. *Journal of Cell Biology* **105**, 949-956 (1987).
- 31 Durand, B., Gao, F. B. & Raff, M. Accumulation of the cyclin-dependent kinase inhibitor p27/Kip1 and the timing of oligodendrocyte differentiation. *Embo J.* **16**, 306-317 (1997).

- 32 Quaroni, A., Tian, J. Q., Seth, P. & Rhys, C. A. p27(Kip1) is an inducer of intestinal epithelial cell differentiation. *Am. J. Physiol.-Cell Physiol.* **279**, C1045-C1057 (2000).
- 33 Hsieh, F. F. *et al.* Cell cycle exit during terminal erythroid differentiation is associated with accumulation of p27(Kip1) and inactivation of cdk2 kinase. *Blood* **96**, 2746-2754 (2000).
- 34 Poluha, W. *et al.* The cyclin-dependent kinase inhibitor p21(WAF1) IS required for survival of differentiating neuroblastoma cells. *Molecular and Cellular Biology* **16**, 1335-1341 (1996).
- 35 Zezula, J. *et al.* p21(cip1) is required for the differentiation of oligodendrocytes independently of cell cycle withdrawal. *EMBO Rep.* **2**, 27-34 (2001).
- 36 Di Cunto, F. *et al.* Inhibitory function of p21(Cip1/WAF1) in differentiation of primary mouse keratinocytes independent of cell cycle control. *Science* **280**, 1069-1072 (1998).
- 37 Egozi, D. *et al.* Regulation of the cell cycle inhibitor p27 and its ubiquitin ligase Skp2 in differentiation of human embryonic stem cells. *Faseb J.* **21**, 2807-2817 (2007).
- 38 Ullmannova, V., Stockbauer, P., Hradcova, M., Soucek, J. & Haskovec, C. Relationship between cyclin D 1 and p21(Waf1/Cip1) during differentiation of human myeloid leukemia cell lines. *Leuk. Res.* **27**, 1115-1123 (2003).
- 39 Bryja, V. *et al.* Lineage specific composition of cyclin D-CDK4/CDK6-p27 complexes reveals distinct functions of CDK4, CDK6 and individual D-type cyclins in differentiating cells of embryonic origin. *Cell Prolif.* **41**, 875-893 (2008).
- 40 Marampon, F. *et al.* Nerve growth factor regulation of cyclin D1 in PC12 cells through a p21(RAS) extracellular signal-regulated kinase pathway requires cooperative interactions between Sp1 and nuclear factor-kappa B. *Mol. Biol. Cell* **19**, 2566-2578 (2008).
- 41 Resnitzky, D. & Reed, S. I. Different roles for Cyclin D1 and Cyclin E in regulation of the G(1)-to-S transition. *Molecular and Cellular Biology* **15**, 3463-3469 (1995).
- 42 Huh, M. S., Parker, M. H., Scime, A., Parks, R. & Rudnicki, M. A. Rb is required for progression through myogenic differentiation but not maintenance of terminal differentiation. *Journal of Cell Biology* **166**, 865-876 (2004).
- 43 Papadimou, E., Menard, C., Grey, C. & Pucoat, M. Interplay between the retinoblastoma protein and LEK1 specifies stem cells toward the cardiac lineage. *Embo J.* **24**, 1750-1761 (2005).
- 44 Thomas, D. M. *et al.* The retinoblastoma protein acts as a transcriptional coactivator required for osteogenic differentiation. *Molecular Cell* **8**, 303-316 (2001).
- 45 Miccadei, S., Provenzano, C., Mojzisek, M., Natali, P. G. & Civitareale, D. Retinoblastoma protein acts as Pax 8 transcriptional coactivator. *Oncogene* **24**, 6993-7001 (2005).
- 46 Hansen, J. B. *et al.* Retinoblastoma protein functions as a molecular switch determining white versus brown adipocyte differentiation. *Proc. Natl. Acad. Sci. U. S. A.* **101**, 4112-4117, doi:10.1073/pnas.0301964101 (2004).

- 47 Neganova, I., Zhang, X., Atkinson, S. & Lako, M. Expression and functional analysis of G1 to S regulatory components reveals an important role for CDK2 in cell cycle regulation in human embryonic stem cells. *Oncogene* **28**, 20-30 (2008).
- 48 Filipczyk, A. A., Laslett, A. L., Mummery, C. & Pera, M. F. Differentiation is coupled to changes in the cell cycle regulatory apparatus of human embryonic stem cells. *Stem Cell Research* **1**, 45-60 (2007).
- 49 Becker, K. A. *et al.* Cyclin D2 and the CDK substrate p220<sup>NPAT</sup> are required for self-renewal of human embryonic stem cells. *Journal of Cellular Physiology* **222**, 456-464.
- 50 Filipczyk AA, L. A., Mummery C, Pera MF. Differentiation is coupled to changes in the cell cycle regulatory apparatus of human embryonic stem cells. *Stem Cell Research* **1**, 45-60 (2007).
- 51 Zhang, X. *et al.* A role for NANOG in G1 to S transition in human embryonic stem cells through direct binding of CDK6 and CDC25A. *Journal of Cell Biology* **184**, 67-82 (2009).
- 52 Card, D. A. G. *et al.* Oct4/Sox2-regulated miR-302 targets cyclin D1 in human embryonic stem cells. *Molecular and Cellular Biology* **28**, 6426-6438 (2008).
- 53 Lee, N. S. *et al.* miR-302b maintains "stemness" of human embryonal carcinoma cells by post-transcriptional regulation of Cyclin D2 expression. *Biochem. Biophys. Res. Commun.* **377**, 434-440 (2008).
- 54 Fenwick, J., Platteau, P., Murdoch, A. P. & Herbert, M. Time from insemination to first cleavage predicts developmental competence of human preimplantation embryos in vitro. *Hum. Reprod.* **17**, 407-412 (2002).
- 55 Kiessling, A. A. *et al.* Evidence that human blastomere cleavage is under unique cell cycle control. *J. Assist. Reprod. Genet.* **26**, 187-195, doi:10.1007/s10815-009-9306-x (2009).
- 56 Borghese, L. *et al.* Inhibition of Notch Signaling in Human Embryonic Stem Cell--Derived Neural Stem Cells Delays G1/S Phase Transition and Accelerates Neuronal Differentiation <I>In Vitro</I> and <I>In Vivo</I>. *Stem Cells* **9999**, N/A.
- 57 Xin Zhang, 2 Irina Neganova,1,2 Stefan Przyborski,1,3 Chunbo Yang,1,2 Michael Cooke,1,3 Stuart P. Atkinson,1,2 George Anyfantis,1,2 Stefan Fenyk,1,3 W. Nicol Keith,4 Stacey F. Hoare,4 Owen Hughes,1,2 Tom Strachan,1,2 Miodrag Stojkovic,1 Philip W. Hinds,5 Lyle Armstrong,1,2 and Majlinda Lako. A role for NANOG in G1 to S transition in human embryonic stem cells through direct binding of CDK6 and CDC25A. *Journal of Cell Biology* **184**, 67–82. (2009).
- 58 Sakaue-Sawano, A. *et al.* Visualizing spatiotemporal dynamics of multicellular cell-cycle progression. *Cell* **132**, 487-498 (2008).
- 59 Karasawa, S., Araki, T., Nagai, T., Mizuno, H. & Miyawaki, A. Cyan-emitting and orange-emitting fluorescent proteins as a donor/acceptor pair for fluorescence resonance energy transfer. *Biochem. J.* **381**, 307-312 (2004).
- 60 Liu, E. B., Li, X. H., Yan, F., Zhao, Q. P. & Wu, X. H. Cyclin-dependent kinases phosphorylate human Cdt1 and induce its degradation. *J. Biol. Chem.* **279**, 17283-17288 (2004).

- 61 Nishitani, H. *et al.* Two E3 ubiquitin ligases, SCF-Skp2 and DDB1-Cul4, target human Cdt1 for proteolysis. *Embo J.* **25**, 1126-1136 (2006).
- 62 Jin, J. P., Arias, E. E., Chen, J., Harper, J. W. & Walter, J. C. A family of diverse Cul4-Ddb1-interacting proteins includes Cdt2, which is required for S phase destruction of the replication factor Cdt1. *Molecular Cell* **23**, 709-721 (2006).
- 63 Arias, E. E. & Walter, J. C. PCNA functions as a molecular platform to trigger Cdt1 destruction and prevent re-replication. *Nat. Cell Biol.* **8**, 84-U33 (2006).
- 64 Higa, L. A. *et al.* L2DTL/CDT2 interacts with the CUL4/DDB1 complex and PCNA and regulates CDT1 proteolysis in response to DNA damage. *Cell Cycle* **5**, 1675-1680 (2006).
- 65 Havens, C. G. & Walter, J. C. Docking of a Specialized PIP Box onto Chromatin-Bound PCNA Creates a Degron for the Ubiquitin Ligase CRL4Cdt2. *Molecular Cell* **35**, 93-104 (2009).
- 66 Guarino, E. *et al.* Cdt1 proteolysis is promoted by dual PIP degrons and is modulated by PCNA ubiquitylation. *Nucleic Acids Res.* (2011).
- 67 Lee, H. O., Zacharek, S. J., Xiong, Y. & Duronio, R. J. Cell Type-dependent Requirement for PIP Box-regulated Cdt1 Destruction During S Phase. *Mol. Biol. Cell* **21**, 3639-3653 (2010).
- 68 Ishii, T. *et al.* Proliferating Cell Nuclear Antigen-dependent Rapid Recruitment of Cdt1 and CRL4Cdt2 at DNA-damaged Sites after UV Irradiation in HeLa Cells. *J. Biol. Chem.* **285**, 41993-42000 (2010).
- 69 Hu, J., McCall, C. M., Ohta, T. & Xiong, Y. Targeted ubiquitination of CDT1 by the DDB1-CUL4A-ROC1 ligase in response to DNA damage. *Nat. Cell Biol.* **6**, 1003-1009 (2004).
- 70 Lydeard, J. R. *et al.* Break-induced replication requires all essential DNA replication factors except those specific for pre-RC assembly. *Genes Dev.* **24**, 1133-1144 (2010).
- 71 Wohlschlegel, J. A. *et al.* Inhibition of eukaryotic DNA replication by geminin binding to Cdt1. *Science* **290**, 2309-+ (2000).
- 72 Wang, S., Ghosh, R. N. & Chellappan, S. P. Raf-1 physically interacts with Rb and regulates its function: a link between mitogenic signaling and cell cycle regulation. *Molecular and Cellular Biology* **18**, 7487-7498 (1998).
- 73 Kinkade, R. *et al.* A Small Molecule Disruptor of Rb/Raf-1 Interaction Inhibits Cell Proliferation, Angiogenesis, and Growth of Human Tumor Xenografts in Nude Mice. *Cancer Res* **68**, 3810-3818 (2008).
- 74 Singh, S. *et al.* Rb-Raf-1 Interaction Disruptor RRD-251 Induces Apoptosis in Metastatic Melanoma Cells and Synergizes with Dacarbazine. *Molecular Cancer Therapeutics* **9**, 3330-3341 (2010).
- 75 Friend, C., Scher, W., Holland, J. G. & Sato, T. Hemoglobin Synthesis in Murine Virus-Induced Leukemic Cells In Vitro: Stimulation of Erythroid Differentiation by Dimethyl Sulfoxide. *Proceedings of the National Academy of Sciences* **68**, 378-382 (1971).
- 76 Terada, M., Nudel, U., Fibach, E., Rifkind, R. A. & Marks, P. A. Changes in DNA associated with induction of erythroid differentiation by dimethyl-sulfoxide in murine erythroleukemia cells. *Cancer Res.* **38**, 835-840 (1978).

- 77 Pulito, V. L., Miller, D. L., Sassa, S. & Yamane, T. DNA fragments in friend-erythro leukemia cells induced by dimethylsulfoxide. *Proceedings of the National Academy of Sciences of the United States of America-Biological Sciences* **80**, 5912-5915 (1983).
- 78 Pantazis, P., Sarin, P. S. & Gallo, R. C. Chromatin conformation during cell differentiation of human myeloid-leukemia cells. *Cancer Letters* **8**, 117-124 (1979).
- 79 Reboulleau, C. P. & Shapiro, H. S. Chemical inducers of differentiation cause conformational changes in the chromatin and deoxyribonucleic acid of murine erythro leukemia cells. *Biochemistry* **22**, 4512-4517 (1983).
- 80 Terada, M., Fried, J., Nudel, U., Rifkind, R. A. & Marks, P. A. Transient inhibition of initiation of S-phase associated with dimethyl sulfoxide induction of murine erythro leukemia cells to erythroid differentiation. *Proceedings of the National Academy of Sciences* **74**, 248-252 (1977).
- 81 Marks, P. A. & Breslow, R. Dimethyl sulfoxide to vorinostat: Development of this histone deacetylase inhibitor as an anticancer drug. *Nat. Biotechnol.* **25**, 84-90, doi:10.1038/nbt1272 (2007).
- 82 Stratling, W. H. STIMULATION OF TRANSCRIPTION ON CHROMATIN BY POLAR ORGANIC-COMPOUNDS. *Nucleic Acids Res.* **3**, 1203-1213 (1976).
- 83 Hebbes, T. R., Thorne, A. W. & Cranerobinson, C. A direct link between core histone acetylation and transcriptionally active chromatin A. *Embo J.* **7**, 1395-1402 (1988).
- 84 Saraiva, N. Z. Histone acetylation and its role in embryonic stem cell differentiation. *World Journal of Stem Cells* **2**, 121, doi:10.4252/wjsc.v2.i6.121 (2010).
- 85 Draper, J. S., Pigott, C., Thomson, J. A. & Andrews, P. W. Surface antigens of human embryonic stem cells: changes upon differentiation in culture. *J. Anat.* **200**, 249-258 (2002).
- 86 Reuben, R. C., Wife, R. L., Breslow, R., Rifkind, R. A. & Marks, P. A. A new group of potent inducers of differentiation in murine erythro leukemia cells. *Proc. Natl. Acad. Sci. U. S. A.* **73**, 862-866 (1976).
- 87 Gambari, R., Marks, P. A. & Rifkind, R. A. Murine erythro leukemia cell differentiation: relationship of globin gene expression and of prolongation of G1 to inducer effects during G1/early S. *Proceedings of the National Academy of Sciences* **76**, 4511-4515 (1979).
- 88 Kiyokawa, H., Richon, V. M., Venta-Perez, G., Rifkind, R. A. & Marks, P. A. Hexamethylenebisacetamide-induced erythro leukemia cell differentiation involves modulation of events required for cell cycle progression through G1. *Proceedings of the National Academy of Sciences* **90**, 6746-6750 (1993).
- 89 Zhuo, S., Fan, S., Huang, S. & Kaufman, S. Study of the role of retinoblastoma protein in terminal differentiation of murine erythro leukemia cells. *Proceedings of the National Academy of Sciences* **92**, 4234-4238 (1995).
- 90 Richon, V. M. *et al.* Two cytodifferentiation agent-induced pathways, differentiation and apoptosis, are distinguished by the expression of human

- papillomavirus 16 E7 in human bladder carcinoma cells. *Cancer Res.* **57**, 2789-2798 (1997).
- 91 Siegel, D. S. *et al.* Hexamethylene bisacetamide induces programmed cell death (apoptosis) and down-regulates BCL-2 expression in human myeloma cells. *Proc. Natl. Acad. Sci. U. S. A.* **95**, 162-166 (1998).
- 92 Baldassarre, G. *et al.* Key role of the cyclin-dependent kinase inhibitor p27(kip1) for embryonal carcinoma cell survival and differentiation. *Oncogene* **18**, 6241-6251 (1999).
- 93 Cecchinato, V. *et al.* Hexamethylene bisacetamide inhibits malignant phenotype in T-ALL cell lines. *Leuk. Res.* **32**, 791-797 (2008).
- 94 Andrews, P. W., Gönczöl, E., Plotkin, S. A., Dignazio, M. & Oosterhuis, J. W. Differentiation of TERA-2 human embryonal carcinoma cells into neurons and HCMV permissive cells. *Differentiation* **31**, 119-126, doi:10.1111/j.1432-0436.1986.tb00392.x (1986).
- 95 Andreeff, M. *et al.* Hexamethylene bisacetamide in myelodysplastic syndrome and acute myelogenous leukemia: a phase II clinical trial with a differentiation-inducing agent. *Blood* **80**, 2604-2609 (1992).
- 96 Rowinsky, E. K. *et al.* Phase 1 and pharmacological study of hexamethylene bisacetamide in patients with advanced cancer. *J. Clin. Oncol.* **4**, 1835-1844 (1986).
- 97 Crnek, V., Vlahovic, M. & Skres, N. Retinoic acid can change normal differentiation of rat egg-cylinders cultured in vitro. *Int. J. DeL Biol.* **35**, 197-202 (1991).
- 98 Mummery, C. L., Vandenbrink, C. E., Vandersaag, P. T. & Delaat, S. W. The cell cycle, cell death, and cell morphology during retinoic acid-induced differentiation of embryonal carcinoma cells. *Dev. Biol.* **104**, 297-307 (1984).
- 99 Mummery, C. L., Vandenbrink, C. E. & Delaat, S. W. Commitment to differentiation induced by retinoic acid in P19 embryonal carcinoma cells is cell cycle dependent. *Dev. Biol.* **121**, 10-19 (1987).
- 100 Mummery, C. L., Vanrooijen, M. A., Vandenbrink, S. E. & Delaat, S. W. Cell cycle analysis during retinoic acid-induced differentiation of a human embryonal carcinoma-derived cell line. *Cell Differentiation* **20**, 153-160 (1987).
- 101 Hui, E. K. W. & Yung, B. Y. M. Cell-cycle phase-dependent effect of retinoic acid on the induction of granulocytic differentiation in HL-60 promyelocytic leukemia cells; evidence for sphinganine potentiation of retinoic acid-induced differentiation. *FEBS Lett.* **318**, 193-199 (1993).
- 102 Freemantle, S. J., Kerley, J. S., Olsen, S. L., Gross, R. H. & Spinella, M. J. Developmentally-related candidate retinoic acid target genes regulated early during neuronal differentiation of human embryonal carcinoma. *Oncogene* **21**, 2880-2889 (2002).
- 103 Baldassarre, G. *et al.* Retinoic acid induces neuronal differentiation of embryonal carcinoma cells by reducing proteasome-dependent proteolysis of the cyclin-dependent inhibitor p27. *Cell Growth Differ* **11**, 517-526 (2000).

- 104 Tonge, P. D. & Andrews, P. W. Retinoic acid directs neuronal differentiation of human pluripotent stem cell lines in a non-cell-autonomous manner. *Differentiation* **80**, 20-30 (2010).
- 105 Simeone, A. *et al.* Sequential activation of HOX2 homeobox genes by retinoic acid in human embryonal carcinoma cells. *Nature* **346**, 763-766 (1990).
- 106 Vlahos, C. J., Matter, W. F., Hui, K. Y. & Brown, R. F. A specific inhibitor of phosphatidylinositol 3-kinase, 2-(4-morpholinyl)-8-phenyl-4H-1-benzopyran-4-one (LY294002). *J. Biol. Chem.* **269**, 5241-5248 (1994).
- 107 Cantley, L. C. The Phosphoinositide 3-Kinase Pathway. *Science* **296**, 1655-1657, doi:10.1126/science.296.5573.1655 (2002).
- 108 Brunet, A. *et al.* Akt Promotes Cell Survival by Phosphorylating and Inhibiting a Forkhead Transcription Factor. *Cell* **96**, 857-868, doi:10.1016/s0092-8674(00)80595-4 (1999).
- 109 Uchida, M. *et al.* FKHL1 inhibits the cell cycle progression of erythroid cells via up-regulation of p27/Kip1. *Experimental Hematology* **30**, 43-43 (2002).
- 110 Paling, N. R. D., Wheadon, H., Bone, H. K. & Welham, M. J. Regulation of Embryonic Stem Cell Self-renewal by Phosphoinositide 3-Kinase-dependent Signaling. *J. Biol. Chem.* **279**, 48063-48070, doi:10.1074/jbc.M406467200 (2004).
- 111 Li, J. *et al.* MEK/ERK signaling contributes to the maintenance of human embryonic stem cell self-renewal. *Differentiation* **75**, 299-307, doi:10.1111/j.1432-0436.2006.00143.x (2007).
- 112 Armstrong, L. *et al.* The role of PI3K/AKT, MAPK/ERK and NF kappa beta signalling in the maintenance of human embryonic stem cell pluripotency and viability highlighted by transcriptional profiling and functional analysis. *Hum. Mol. Genet.* **15**, 1894-1913, doi:10.1093/hmg/ddl112 (2006).
- 113 McLean, A. B. *et al.* Activin efficiently specifies definitive endoderm from human embryonic stem cells only when phosphatidylinositol 3-kinase signaling is suppressed. *Stem Cells* **25**, 29-38 (2007).
- 114 Desbordes, S. C. *et al.* High-throughput screening assay for the identification of compounds regulating self-renewal and differentiation in human embryonic stem cells. *Cell Stem Cell* **2**, 602-612 (2008).
- 115 Watanabe, K. *et al.* A ROCK inhibitor permits survival of dissociated human embryonic stem cells. *Nat Biotech* **25**, 681-686 (2007).
- 116 Damoiseaux, R., Sherman, S. P., Alva, J. A., Peterson, C. & Pyle, A. D. Integrated Chemical Genomics Reveals Modifiers of Survival in Human Embryonic Stem Cells. *Stem Cells* **27**, 533-542 (2009).
- 117 Xu, Y. *et al.* Revealing a core signaling regulatory mechanism for pluripotent stem cell survival and self-renewal by small molecules. *Proceedings of the National Academy of Sciences* **107**, 8129-8134 (2010).
- 118 Andrews, Paul D. *et al.* High-content screening of feeder-free human embryonic stem cells to identify pro-survival small molecules. *Biochem. J.* **432**, 21-33 (2010).
- 119 Fazio, T. G., Huff, J. T. & Panning, B. An RNAi screen of chromatin proteins identifies Tip60-p400 as a regulator of embryonic stem cell identity. *Cell* **134**, 162-174 (2008).

- 120 Ding, L. *et al.* A Genome-Scale RNAi Screen for Oct4 Modulators Defines a Role of the Paf1 Complex for Embryonic Stem Cell Identity. *Cell Stem Cell* **4**, 403-415 (2009).
- 121 Gonzalez, R. *et al.* Screening the mammalian extracellular proteome for regulators of embryonic human stem cell pluripotency. *Proc. Natl. Acad. Sci. U. S. A.* **107**, 3552-3557 (2010).
- 122 Mayshar, Y., Yanuka, O. & Benvenisty, N. Teratogen screening using transcriptome profiling of differentiating human embryonic stem cells. *J. Cell. Mol. Med.* **15**, 1393-1401 (2011).
- 123 Chang, K. H. & Zandstra, P. W. Quantitative screening of embryonic stem cell differentiation: Endoderm formation as a model. *Biotechnology and Bioengineering* **88**, 287-298 (2004).
- 124 Ho, H. Y. & Li, M. Potential application of embryonic stem cells in Parkinson's disease: drug screening and cell therapy. *Regen. Med.* **1**, 175-182 (2006).
- 125 McNeish, J. *et al.* High-throughput Screening in Embryonic Stem Cell-derived Neurons Identifies Potentiators of alpha-Amino-3-hydroxyl-5-methyl-4-isoxazolepropionate-type Glutamate Receptors. *J. Biol. Chem.* **285**, 17209-17217 (2010).
- 126 Thomson, J. A. *et al.* Embryonic Stem Cell Lines Derived from Human Blastocysts. *Science* **282**, 1145-1147, doi:10.1126/science.282.5391.1145 (1998).
- 127 Costa, M. *et al.* A method for genetic modification of human embryonic stem cells using electroporation. *Nat. Protoc.* **2**, 792-796, doi:10.1038/nprot.2007.105 (2007).
- 128 D'Amour, K. A. *et al.* Production of pancreatic hormone-expressing endocrine cells from human embryonic stem cells. *Nat Biotech* **24**, 1392-1401 (2006).
- 129 Kim, D.-S. *et al.* Robust Enhancement of Neural Differentiation from Human ES and iPS Cells Regardless of their Innate Difference in Differentiation Propensity. *Stem Cell Reviews and Reports* **6**, 270-281 (2010).
- 130 Cerdan, C., Hong, S.H. & Bhatia, M. . Formation and hematopoietic differentiation of human embryoid bodies by suspension and hanging drop cultures. *Current protocols in stem cell biology* (2007).
- 131 Kanda, T., Sullivan, K. F. & Wahl, G. M. Histone GFP fusion protein enables sensitive analysis of chromosome dynamics in living mammalian cells. *Current biology : CB* **8**, 377-385 (1998).
- 132 Niwa, H., Yamamura, K. & Miyazaki, J. Efficient selection for high-expression transfectants with a novel eukaryotic vector. *Gene* **108**, 193-199 (1991).
- 133 de Felipe, P., Hughes, L. E., Ryan, M. D. & Brown, J. D. Co-translational, intraribosomal cleavage of polypeptides by the foot-and-mouth disease virus 2A peptide. *J. Biol. Chem.* **278**, 11441-11448 (2003).
- 134 Thomas, N. *et al.* Characterisation and Gene Expression Profiling of a Stable Cell Line Expressing a Cell Cycle GFP Sensor. *Cell Cycle* **4**, 191-195 (2005).
- 135 Neganova, I. & Lako, M. Cell cycle regulation in human embryonic stem cells. *J. Anat.* **212**, 76-76 (2008).

- 136 Ghule, P. N. *et al.* Cell cycle dependent phosphorylation and subnuclear organization of the histone gene regulator p220(NPAT) human in embryonic stem cells. *Journal of Cellular Physiology* **213**, 9-17 (2007).
- 137 Neganova, I. & Lako, M. 30-44 (Blackwell Publishing).
- 138 Henderson, J. K. *et al.* Preimplantation human embryos and embryonic stem cells show comparable expression of stage-specific embryonic antigens. *Stem Cells* **20**, 329-337 (2002).
- 139 O'Connor, M. D. *et al.* Alkaline Phosphatase-Positive Colony Formation Is a Sensitive, Specific, and Quantitative Indicator of Undifferentiated Human Embryonic Stem Cells. *Stem Cells* **26**, 1109-1116 (2008).
- 140 Shimozaki, K. Involvement of Oct3/4 in the enhancement of neuronal differentiation of ES cells in neurogenesis-inducing cultures. *Development* **130**, 2505-2512 (2003).
- 141 Cimadamore, F. *et al.* Human ESC-Derived Neural Crest Model Reveals a Key Role for SOX2 in Sensory Neurogenesis. *Cell Stem Cell* **8**, 538-551 (2011).
- 142 Yang, Valerie S. *et al.* Geminin Escapes Degradation in G1 of Mouse Pluripotent Cells and Mediates the Expression of Oct4, Sox2, and Nanog. *Curr. Biol.* **21**, 692-699 (2011).
- 143 Becker, K. A., Stein, J. L., Lian, J. B., Van Wijnen, A. J. & Stein, G. S. Human Embryonic Stem Cells Are Pre-Mitotically Committed to Self-Renewal and Acquire a Lengthened G1 Phase Upon Lineage Programming. *Journal of Cellular Physiology* **222**, 103-110 (2010).
- 144 Lumelsky, N. *et al.* Differentiation of Embryonic Stem Cells to Insulin-Secreting Structures Similar to Pancreatic Islets. *Science* **292**, 1389-1394 (2001).
- 145 Blyszczuk, P. *et al.* Expression of Pax4 in embryonic stem cells promotes differentiation of nestin-positive progenitor and insulin-producing cells. *Proceedings of the National Academy of Sciences* **100**, 998-1003 (2003).
- 146 Reubinoff, B. E. *et al.* Neural progenitors from human embryonic stem cells. *Nat. Biotechnol.* **19**, 1134-1140 (2001).
- 147 Evseenkoa, D. *et al.* Mapping the first stages of mesoderm commitment during differentiation of human embryonic stem cells. *Proceedings of the National Academy of Sciences* **107**, 13742-13747 (2010).
- 148 Vallier, L. *et al.* Signaling Pathways Controlling Pluripotency and Early Cell Fate Decisions of Human Induced Pluripotent Stem Cells. *Stem Cells* **27**, 2655-2666 (2009).
- 149 Meriin, A. B., Gabai, V. L., Yaglom, J., Shifrin, V. I. & Sherman, M. Y. Proteasome Inhibitors Activate Stress Kinases and Induce Hsp72. *J. Biol. Chem.* **273**, 6373-6379 (1998).
- 150 Yamaguchi, R. & Dutta, A. Proteasome inhibitors alter the orderly progression of DNA synthesis during S-phase in HeLa cells and lead to rereplication of DNA. *Exp. Cell Res.* **261**, 271-283 (2000).
- 151 Finley, D. *et al.* Inhibition of proteolysis and cell cycle progression in a multiubiquitination-deficient yeast mutant. *Mol. Cell. Biol.* **14**, 5501-5509 (1994).

- 152 Sherwood, S. W., Kung, A. L., Roitelman, J., Simoni, R. D. & Schimke, R. T. In vivo inhibition of cyclin B degradation and induction of cell-cycle arrest in mammalian cells by the neutral cysteine protease inhibitor N-acetylleucylleucylnorleucinal. *Proceedings of the National Academy of Sciences* **90**, 3353-3357 (1993).

